
Self-Driving Datasets: From 20 Million Papers to Nuanced Biomedical Knowledge at Scale

Haydn Jones¹ Yimeng Zeng¹ Alden Rose¹ Li S. Yifei¹ Yining Huang¹
Kaiwen Wu¹ Jiaming Liang¹ Maggie Ziyu Huan¹ Yoseph Barash² Cesar de la Fuente-Nunez³
Osbert Bastani¹ Zachary Ives¹ Mark Yatskar^{1,*} Jacob R. Gardner^{1,*}

¹Department of Computer and Information Science, University of Pennsylvania

²Department of Genetics, University of Pennsylvania

³Departments of Bioengineering and Chemical and Biomolecular Engineering,
University of Pennsylvania

*Equal contribution

Abstract

Manually curated biomedical repositories—spanning bioactivity, genomics, and chemistry—are expensive to maintain, lag behind primary literature, and often discard experimental context. The absence of contextual information obscures critical nuances, thereby complicating the assessment of data correctness and coverage, necessary criteria for building high-quality models. We show that PubMed itself can be turned into structured datasets—autonomously and cost-effectively—that are larger, more nuanced, and more accurate than the curated databases they would replace. We present three coupled contributions: (1) an LLM-based entity-tagging pipeline, grounded in nine biomedical ontologies, that tags 4.5 billion entities across 19 categories in a 22.5M-paper, 2.5-trillion-token PubMed corpus; (2) hybrid sparse–dense retrieval infrastructure supporting surgical entity-filtered semantic queries over the tagged corpus; and (3) *Starling*, a multi-agent deep research system that, given only a natural-language task description, autonomously designs precision- and recall-targeted retrieval filters, induces an extraction schema, and emits structured records with nuance-rich fields and supporting passages. Applied to six tasks—blood-brain barrier permeability, oral bioavailability, acute toxicity (LD50), gene–disease associations, protein subcellular localization, and chemical reactions—*Starling* produces ~ 6.3 M records (per-task scale ranges from 91K to 3M); several of these are, to our knowledge, the largest public datasets for their respective properties. Frontier-model rejection of our kept extractions is 0.6–7.7% across tasks, surprisingly far below the error rates we measure on the widely used, manually curated counterparts (e.g., 16.5% on *BBB_Martins*, 7.3% on *Bioavailability_Ma*). Beyond scale and accuracy, the attached supporting passages carry nuance that tabular databases discard: for example, oral bioavailability of a molecule might depend on whether the patient is fed or fasted. Together, the corpus, retrieval layer, and agent establish a foundation for multimodal predictive and generative models in AI-driven therapeutic design. We release code and links to our datasets at <https://github.com/starling-labs/starling>.

1 Introduction

For decades, the biomedical sciences have invested heavily in the collection, curation, and dissemination of experimental data. This investment has paid off: centralized repositories have enabled rapid and widely successful applications of AI and machine learning across genomics, protein folding, medical and laboratory imaging, and drug discovery [21, 20, 61]. However, much of this data is captured manually at tremendous cost and aggregated into structured, tabular databases [17, 24, 22].

Preprint.

The dominant use case for these collections is the familiar pattern of supervised learning: given input features, predict a label. Even recent generative applications are primarily unimodal: given a protein’s primary structure, generate its folded structure or a novel binder.

The success of this paradigm is difficult to overstate. But the ability of modern large language models to extract nuanced information directly from unstructured text [46, 36, 67] exposes three shortcomings of existing biomedical data repositories that are increasingly difficult to ignore:

1. *Existing data lacks nuance.* Most medically relevant properties are not functions of the molecule alone. Oral bioavailability depends on whether a drug is taken on an empty stomach, the formulation it is delivered in, and the population it is dosed in; reaction yields depend on procedure and conditions; assay readouts depend on cell line and protocol. Models that operate unimodally on the molecule can at best estimate the marginal distribution over these conditions. Text makes the conditions themselves first-class.
2. *Existing data is incomplete.* Repositories lag the literature by years, and even at steady state they capture a small fraction of what has been measured: datasets could plausibly grow by orders of magnitude. Worse, evidence for the same physical phenomenon is often reported in incompatible forms. Hepatotoxicity may surface as binding to a liver enzyme or as a population-level adverse-event signal; oral bioavailability may be reported in absolute terms or relative to a reference compound. These are awkward to flatten into a single schema but easy to describe in language.
3. *Existing data is less accurate than commonly assumed.* When we audit widely used benchmarks against human judgment (Section 5.2), we find non-trivial label error: 16.5% on TDC BBB and 7.3% on TDC Oral Bioavailability [17]. Models trained on these labels inherit that error as a noise floor and a ceiling on achievable test performance.

The natural response to these shortcomings is to go back to the source. The primary literature contains, in principle, both the missing data and the experimental context that tabular schemas discard—and unlike a curated database, it grows continuously. Historically, the obstacle has been access: extracting structured records from tens of millions of papers requires a kind of surgical retrieval that neither classical information extraction nor recent deep research agents are equipped to perform. General-purpose deep research agents are designed to synthesize relevant documents into a narrative report, not to exhaustively sweep a corpus for every instance of a phenomenon and emit a structured record [18, 41].

In this paper we present a system that does exactly this. It operates over a tagged and indexed corpus of 22.5 million PubMed papers and answers natural-language extraction tasks of the form “*find all examples in the corpus where the oral bioavailability of a small molecule is discussed*” or “*find all instances where evidence of any gene-disease association is presented.*” Given only a task description, the system autonomously designs retrieval filters combining entity constraints and semantic queries, induces an extraction schema, and outputs structured records linked to supporting passages in the source paper. This enables the construction of large, nuanced, literature-grounded datasets in days, replacing years of manual curation, and our audits show this can be done at even higher accuracy.

Our specific contributions are:

1. **A method for self-driving biomedical dataset construction.** We introduce *Starling*, a multi-agent deep research system that autonomously designs and extracts structured records from the literature. *Starling* operates over a tagged and indexed corpus, supported by two components we develop alongside it: an entity tagging model fine-tuned from `gpt-oss-20b` [1] covering 19 top-level biomedical categories, grounded in nine reference ontologies and, for small molecules and proteins, directly to SMILES and amino acid sequences; and a hybrid sparse–dense retrieval layer that exposes the tagged corpus through entity-filtered semantic queries.
2. **Evidence that automated extraction can exceed manual curation in size, accuracy, and nuance.** Across six therapeutic discovery tasks, *Starling* yields ~ 6.3 M judge-filtered records, including several that are, to our knowledge, the largest public datasets for their properties. Frontier-model and human audits estimate per-task error at 0.6–4.7%, below our estimates for widely used manually curated benchmarks. Supporting passages add signal beyond structure-only representations: for a given molecule, residual variation in oral bioavailability is often significantly explained by experimental context (e.g., fed vs. fasted dosing). Existing deep research systems either fail on these extraction tasks or mainly rediscover scientist-curated datasets.

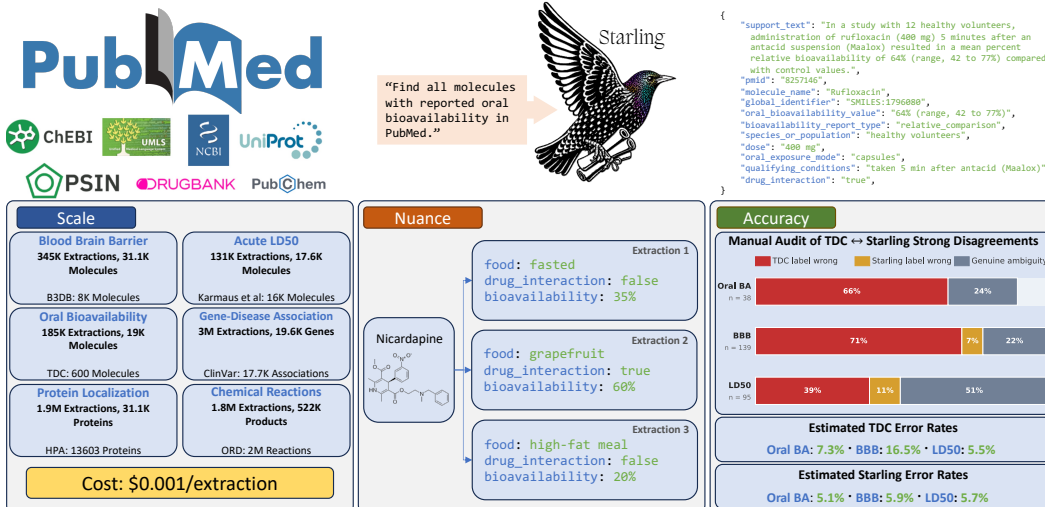


Figure 1: Starling is a promptable agentic system that automatically creates datasets from biomedical literature. Starling is fully self-driving, requiring no human intervention, and produces datasets at comparable or larger scale than manual resources, capturing nuanced context often missing in existing datasets, with similar or better accuracy. Starling can keep datasets better synchronized to quickly expanding information in literature, at under 1 cent per datum it extracts.

3. **Open release of the system, recipes, and datasets.** We open-source the Starling agent, entity tagging model, retrieval infrastructure, and end-to-end recipes for reproducing the pipeline on any suitably licensed corpus, and provide open access to the system running on our own licensed corpus. We also release six datasets covering small-molecule blood-brain barrier permeability, oral bioavailability, acute toxicity (LD50), gene-disease associations, protein subcellular localization, and chemical reactions. See Appendix A for details on our release plans.

2 Corpus and Database Construction

We use a corpus of 22.5 million PubMed articles. This corpus represents the subset of PubMed available to us with (1) journal licensing terms that do not preclude AI usage and (2) relatively straightforward pathways to acquire PDFs. We extract text and tables into markdown files using `dots.ocr` [29]. In this work, we do not yet consider the information contained in figures. This results in a corpus of approximately 2.5 trillion tokens, which we divide into overlapping chunks of 5 paragraphs and embed with `Qwen3-Embedding-4B` [66], creating an initial database of roughly 250 million 1024-dimensional embedding vectors. In contrast to traditional RAG and deep research agents [34, 57, 55], our system uses these embeddings to *re-rank* search results rather than filter the corpus.

Challenges for self-driving datasets. Consider an extraction task such as “find a large set of molecules for which blood-brain barrier permeability is discussed.” At 2.5 trillion tokens, a linear pass over the full corpus per task is prohibitively expensive, even with a fast LLM, ruling out brute-force extraction. Existing deep research agents [34, 57, 55] synthesize reports from a small set of retrieved documents rather than exhaustively scanning a corpus. Embedding-based retrieval can surface relevant passages, but at corpus scale it is a noisy *filter* and works better as a passage *re-ranker*. We need a cheap filtering mechanism that narrows tens of millions of papers to manageable subsets likely to contain the target data.

Entity tagging enables this: for molecule-related tasks, we focus only on chunks that mention at least one small molecule, discarding most of the corpus. However, extraction tasks are not known in advance—a future query may seek gene-disease associations or reaction yields, each needing different entity co-occurrences. The tagging layer must therefore span a broad range of biomedical entity types so downstream agents can compose arbitrary entity filters on demand.

2.1 Entity Tagging

We tag the corpus with 19 top-level biomedical entity types—`SmallMolecule`, `Gene`, `Disease`, `Protein`, and others (see Appendix G)—grounded in nine reference ontologies. Recent work shows that LLMs can outperform BERT-style taggers on biomedical NER [46, 36, 67], motivating the teacher–student pipeline below. Each paragraph in the resulting corpus carries canonical, ontology-linked entity tags that downstream agents can compose into arbitrary entity filters.

Tag schema. The teacher labels a window of 3 consecutive paragraphs with a list of entity tags. Each tag includes a disambiguated canonical name selected by the model, the entity type, optional synonyms to aid normalization, the exact surface forms in the text, and the subset of paragraphs in which the entity is mentioned. Type-specific optional fields capture organism specificity (e.g., *Homo sapiens* for genes and proteins), medicinal-chemistry aliases (e.g., 6f), and resolved names (e.g., the IUPAC name for a small molecule).

Normalization. After tagging, each extracted entity is grounded to a reference ontology. UMLS [9] is our default, covering `Disease`, `Anatomy`, `Phenotype`, `GOTerm`, and most other concept types via aggregated biomedical ontologies; when using other ontologies, we follow the UMLS free-text-to-concept matching pipeline¹. Where more authoritative domain resources exist, we instead use a cascade of OPSIN [31], DrugBank [26], ChEBI [15], and PubChem [24] (in that order) for `SmallMolecule`; ChEBI for `SmallMoleculeClass`; NCBI Taxonomy [52] for `Organism`; UniProt [4] for `Protein`; and NCBI Gene [12] for `Gene`.

Distillation pipeline. We sample 50,000 papers and run `gpt-oss-120b` [1] 19 times per window—once per entity type—using a standardized, type-specific prompt with its own rules and few-shot examples. Running separate single-type passes lets the model focus on one category at a time, improving precision and recall over a joint 19-type pass. Before training the student model, we validate the 1,000 most frequent entities per type by mapping them to a reference ontology and selecting the 10 most likely candidates. GPT-5 [54] then chooses the correct candidate (or rejects all), and we replace the teacher’s tags with the ontology’s preferred names and synonyms, enforcing consistent nomenclature for high-frequency concepts. We then merge tags across types within each window to obtain windows labeled with all 19 types and fine-tune `gpt-oss-20b` on this combined supervision. The distilled student is run on the full 22.5M-paper corpus and its outputs are re-normalized (without GPT-5 validation, which is used only at distillation time), as the larger corpus surfaces entities missing from the 50,000-paper sample.

2.2 Constructing Entity Filters

The deep research agents we construct next interact with our tagged corpus primarily by using *entity filters* that select subsets of the corpus, which we then re-rank with a semantic query—for example, “search only over windowed chunks in the corpus that mention both some small molecule and the blood-brain barrier.” Each filter is represented as a `FilterSpec` containing a CNF entity constraint (outer conjunction, inner disjunction, with negation support via prefix notation). We provide a simple example of a filter specification and a discussion of how it is used in Appendix G.

3 Deep Research Agents for Self-driving Datasets

To convert the tagged corpus into structured datasets, we introduce `Starling`, a multi-agent deep research system that turns a natural-language task description into a structured dataset, requiring no user-specified schema and no manual paper selection.

Literature-scale extraction faces two main challenges. First, we cannot make linear passes over the 2.5T-token corpus for each task, so we must choose which subset of the literature to process and in what order. Second, if the LLM is free to invent fields on each extraction, hundreds of thousands of extractions will produce an unusably inconsistent schema. Thus, beyond universal fields like `PMID` and `support_text`, we must predefine a set of relevant structured fields (e.g., `fed_or_fasted` for oral bioavailability) based on domain knowledge. To address this, `Starling` runs in two phases. During *query construction*, we filter and reorder the corpus and inspect matching papers to design the extraction schema. During *extraction*, we process this subcorpus to perform the extractions.

¹See https://www.nlm.nih.gov/research/umls/implementation_resources/query_diagrams/index.html for details on UMLS term normalization.

3.1 Phase 1: Query Construction

A `Proposer` agent constructs a set of **probes** $\{P_1, \dots, P_T\}$. Each probe consists of (1) an entity filter (Section 2.2) and (2) a semantic query. Each probe ideally targets a distinct yet relevant portion of the corpus, achieving high precision and recall on minimally overlapping subsets. The agent explores the corpus with tools that run semantic search on entity-filtered subsets to form initial probe specifications, then iteratively creates probes to maximize estimated precision and recall.

Maximizing precision. Each text matched by probe P_i should yield a relevant extraction as often as possible. To estimate this precision, the agent samples papers from a probe’s filter and tasks a `Validator` agent to judge what fraction is relevant. An `Investigator` agent examines text that the `Validator` deems irrelevant but passes the filter. It suggests strategies to refine the probe that would exclude these irrelevant results while minimally impacting relevant ones.

Maximizing recall. The union of our probes should ideally filter out minimally relevant text. To estimate recall, we need to check how often we can find relevant extractions in papers that our probes currently *exclude*. To do this, we look at chunks that are highly relevant according to the T semantic queries but are excluded by all T entity filters. The `Validator` judges each chunk, and the fraction marked relevant is our **recall-gap estimate**. If this fraction is high, it means it is “easy” to find relevant text that our current probe set excludes. To fix this, the `Proposer` must either make some probe more permissive or construct a new probe P_{t+1} , guided by `Investigator` suggestions, that captures relevant text missed by P_1, \dots, P_t .

This process repeats. At each iteration, the `Proposer` uses (1) precision and recall estimates, and (2) `Investigator` feedback to modify existing probes or construct additional probes to capture the gaps identified. We continue refining until we estimate 80% precision and at most a 15% recall gap, or until a maximum number of probes is reached. See Appendix F for more details.

Schema induction. After selecting probes P_1, \dots, P_T , we define a shared extraction schema for all dataset rows. The `Proposer` samples a few retrieval-set papers and runs the `Extractor` (described below) *without* a fixed schema. From the resulting free-form records, the agent derives a unified schema with field names, types, allowed values, and a concrete *task instantiation* specifying what counts as a valid record, what to ignore, and what default assumptions to use. For the blood-brain barrier task, the instantiation requires a named compound and an explicit permeability statement, assuming an intact barrier by default (so a diseased state becomes a qualifying condition). The `Validator` scores extraction quality under the proposed schema; if it is below target, the `Proposer` revises and the loop repeats. Once quality meets the target, the schema and instantiation are frozen and applied to the full retrieval set. At this stage, a human can intervene to shape the probes or extraction schema (e.g., in our `Reactions` task, we skip schema construction and use a hand-authored schema that roughly matches the one used by the Open Reaction Database in Section 5).

3.2 Phase 2: Extraction

Once the `Proposer` returns a retrieval specification, we execute it against the corpus to produce the set of matching papers and then rank papers by (1) semantic similarity and (2) the number of probe filters they match. Extraction is substantially more straightforward than planning: an `Extractor` agent loops over windows from the ordered subcorpus implied by the probe set and emits extractions using the instructions and schema that were generated during query construction.

Because the `Extractor` runs once per window without a global view, the deduplicated set still includes off-task, mis-attributed, or low-fidelity rows. A `Judge` filters these as the final pipeline stage. After completing the extraction pipeline for a task, we use GPT-5.4 to score a small sample of extractions along five axes: *task relevance* (the record matches the task), *primary-label correctness* (the headline value matches the source), *span fidelity* (the supporting passage contains the claim), *secondary-field accuracy* (auxiliary fields match the passage), and *entity attribution* (the primary entity is correctly identified and resolved). We then distill these judgments into a Qwen3.5-9B model using SFT and GRPO [53] across all six tasks. A record is kept only if it passes all five axes. Section 5.2 reports per-task pass rates and the rate at which frontier models reject kept entries. See Appendix F for more details on the judgment pipeline.

4 Experimental Setup

Case Studies. We evaluate Starling on six therapeutically relevant tasks (Fig. 3): three small-molecule properties—blood-brain barrier permeability (BBB), oral bioavailability (Oral), and LD50—plus gene-disease associations (GDA), protein subcellular localization (PSL), and chemical reactions (Reactions). Each dataset record includes a primary entity, a target measurement, structured task-specific fields, and a free-text supporting passage. While the Extractor (Section 3.2) induces schemas autonomously, for Reactions we manually authored the schema and per-field extraction guidance to enable direct comparisons with ORD.

Baselines. To assess the reliability of Starling datasets, we align each case study with an existing benchmark: TDC for BBB, Oral, and LD50 [17]; B3DB for BBB [40]; ClinVar for GDA [27]; UniProt (*Homo sapiens* only) for PSL [4]; and the Open Reaction Database (ORD) for Reactions [22]. We compare these on accuracy, size, and cost, and benchmark against existing deep research systems in Section 5.3 and Appendix B. We also quantify the downstream effects of training with Starling data. Our base predictor is MiniMol [25], a supervised model trained on TDC data and outputs from a physical simulator that is currently state-of-the-art on a range of tasks.

5 Results

We organize the rest of this section around three main claims: Starling’s extractions are large in scale and effective as training data (Section 5.1), accurate—and even *more accurate* than the manually curated benchmarks they extend (Section 5.2), and outperform existing deep-research agents for dataset curation while being cost-effective (Section 5.3).

5.1 Starling Datasets are Large-Scale and Drive Effective Model Training

Table 1: Per-task extraction counts collected by Starling, alongside error rates from two strong LLM evaluators measuring the fraction of extractions that fail at least one evaluation axis.

Task	Starling Statistics			Dataset Comparisons		Error Rate	
	Extractions	Papers	Unique IDs	Coverage	Scale	Opus 4.7	GPT-5.4
BBB	304K	122K	31.1K	44.3% TDC	4x B3DB	4.05%	5.88%
GDA	3.00M	145K	19.6K	41.9% ClinVar	6x ClinVar	0.88%	5.70%
LD50	91K	30.3K	17.6K	31.5% TDC	2x TDC	3.89%	5.72%
Oral	163K	45.0K	19.0K	96.1% TDC	29x TDC	0.56%	5.06%
PSL	1.79M	171K	36.1K	90.8% UniProt	24x UniProt	1.12%	5.56%
Reactions	916K	259K	545K	—	0.51x ORD	4.68%	7.78%

Starling Dataset Sizes. In Table 1 we report, for each case study, the total number of extractions Starling produces and how they compare to existing resources. We compare datasets in two ways: (1) how many instances from existing resources we cover (Coverage), and (2) overall size (Scale). Across all case studies, Starling produces datasets as large as existing resources while maintaining high coverage. While the literature does not cover every instance in the manually curated resources, Starling’s extractions remain more up to date than these resources. In reactions, we discover nearly half a million new products not yet described in public datasets (Appendix C.1).

Using Starling datasets to augment property prediction. In Table 2, we consider how useful Starling-curated data is for training and evaluating models. Starting with MiniMol [25], we first fine-tune it on manually curated TDC datasets and evaluate on TDC test data or Starling-derived test data. Then, we evaluate the effect of augmenting training data with Starling instances chosen using a train/test splitting mechanism similar to TDC’s (Aug), comparing test performance with and without augmentation. Across the three TDC-backed case studies, augmenting predictor training with Starling data never substantially hurts performance and often improves it, both on diverse literature-sourced data and on manually curated test sets.

Cost. Across the six tasks, end-to-end Starling extractions cost approximately \$0.001 per record on average, dominated by inference costs for extraction. Distilling and training the judge was a one-time cost of approximately \$400, amortized across the six tasks.

Table 2: Predictive performance on (1) the TDC test set with and without additional training data extracted from the literature, and (2) on a new literature extracted test set

Task	Metric	TDC Test	TDC Test (Aug.)	Lit. Test	Lit. Test (Aug.)
Oral Bioavailability	AUROC \uparrow	0.692	0.779	0.768	0.821
LD50	MAE \downarrow	0.602	0.575	0.650	0.641
BBB	AUROC \uparrow	0.916	0.909	0.768	0.890

5.2 Starling Datasets Are Accurate and Often Surpass Manual Curation

Table 3: Human-validated label error rates on molecules in four manually curated databases where Starling found ≥ 3 extractions. We hand-judged the disagreement subset (majority of Starling extractions disagree with the database label, or > 0.5 log units of disagreement for LD50), reviewing 8,765 extractions in total. The **confirmed-wrong** columns considers all ≥ 3 -extraction molecules; e.g., the B3DB row reflects 1086 total molecules, of which $214/1086 = 19.7\%$ were judged mislabeled. Both rates are lower bounds: molecules whose Starling extractions agreed with the database label were not audited and are presumed correct.

Baseline Dataset	Mols. Reviewed	Baseline wrong	Starling wrong	Lit. ambiguous	Confirmed-wrong baseline rate	Confirmed-wrong Starling rate
Bioavailability_Ma	34	25	0	9	7.3%	0.0%
BBB_Martins	138	98	10	30	16.5%	1.7%
LD50_Zhu	95	37	10	48	5.5%	1.5%
B3DB	316	214	20	78	19.7%	1.8%

Human calibration of the LLM judge. We first verify that an LLM judge is a reasonable proxy for human review on the five axes (Section 3.2). Six annotators independently reviewed BBB and LD50 extractions, scoring each. For each task, 20 extractions were shared across all reviewers (for inter-annotator agreement), and each reviewer labeled 5 additional unique extractions, yielding 50 total extractions per task. Human pass rates were 97.3% on BBB and 94.0% on LD50, matching the frontier-judge pass rates in Table 1. Judge-human agreement on the shared subset (95.8% BBB, 92.0% LD50) is within about one percentage point of human-human agreement (95.1% BBB, 90.6% LD50), indicating that the LLM judge is as consistent with annotators as they are with each other.

Judge results. With the LLM judge thus calibrated, we evaluated at least 3,000 kept extractions per task with two frontier judges, reporting the rate at which each flags an extraction as failing on at least one axis (Table 1). Both judges report error rates below 10% on every task, typically at or below 5%.

Comparing Starling accuracy to existing resources. We compare Starling to four manually curated databases, considering only molecules with at least three Starling extractions. This threshold lets us label each case as correct, ambiguous, or wrong, rather than as a binary correct/incorrect. We manually reviewed molecules where the majority of Starling extractions disagreed with the database; cases where the majority agreed were treated as confirming the database label. Annotators investigated each disagreement and read Starling’s supporting documents to judge whether the database label was correct (Table 3). Most disagreements were database errors: every resource had a confirmed-wrong rate above 5%, and B3DB exceeded 19%. Using the same denominator, Starling’s confirmed-wrong rate is $\leq 1.8\%$, indicating that its extractions are at least as accurate as these curated datasets, and often more so. For selected “clear” errors, see Table 12.

5.3 Starling is a Higher-Quality Data Generator Than Frontier Deep Research Systems

We evaluate how five frontier deep research systems handle dataset-construction requests: BioMNI-Phylo (a sandboxed Python coding agent) [18], Claude Research Mode (Opus 4.6 Extended), GPT-5.4 Deep Research, GPT-5.4 Pro Extended Thinking, and Kosmos AI-Scientist (Edison Scientific) [41]. Many of these produce narrative construction plans rather than data, so we passed these plans to Claude Code for execution. Manual inspection reveals three main strategies: (1) reformatting existing curated databases; (2) small-scale PubMed text mining with high false-positive rates; and (3) catastrophically invalid bulk extraction at scale. None produce datasets that are simultaneously large, paper-derived, and high-precision—consistent with the fact that their agentic designs are ill-suited

Table 4: Literature-grounded record counts per task: the strongest deep-research baseline *for that task* vs. Starling. A row counts as “literature-grounded” if it carries a real PMID (or an upstream-dataset PMID we recovered for the agent; rescue methodology in Appendix B.4); we credit baselines at face value with no per-row LLM judging. Starling counts are post-judge-filter (Table 1); baseline counts are unfiltered. GPT-5.4 Deep Research is strongest on T1; Kosmos AI-Scientist is strongest on T2/T4/T5 and ties GPT-5.4 Deep Research on T3 (both consume the same PubTator3 BioREx file). See more details in Appendix B, and full per-agent breakdown in Appendices B.3 and B.4.

Task	Strongest baseline	Baseline rows	Starling (judge-filtered)
BBB	GPT-5.4 Deep Research	10,990	304,845
Oral	Kosmos AI-Sci.	30,308	163,815
GDA	Kosmos / GPT-5.4 Deep Res.*	1,455,774	3,009,161
LD50	Kosmos AI-Sci.	56,658	91,597
PSL	Kosmos AI-Sci.	180,685	1,798,418

to this task. In Table 4, we compare to, for each task, the deep research system with the largest number of correctly formatted, literature-grounded instances. We assume baseline output is correct and compare on scale (Appendices B.2 and B.4 has per-agent strategies and statistics).

6 Starling Builds Contextualized Data Enabling Nuanced Predictions

Starling curates rich, high-signal, property-altering context for each extraction. This context captures the conditions under which properties change, encodes human understanding of mechanisms of action, and surfaces free-text information tied to each measurement. For example, a drug’s oral bioavailability can vary greatly with food intake and meal characteristics (e.g., Nicardipine in Fig. 1). Such nuance has been largely overlooked by dataset designers. During information extraction, Starling collects two kinds of context: (1) named fields with values from a fixed set, and (2) unstructured supporting text that provides context and justifies those values. Even in data settings that collect context, it is often very incomplete and Starling systematically finds more (Appendix C.2).

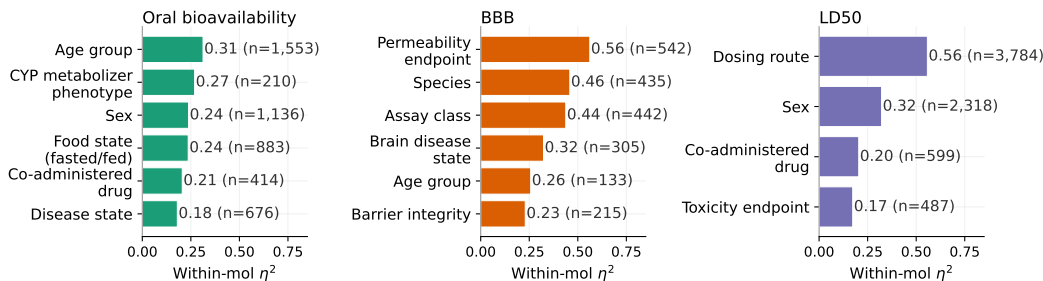


Figure 2: Within-mol η^2 ANOVA effect size statistics for each task / conditioning variable: the fraction of a molecule’s label variance explained by that single covariate, averaged across molecules with ≥ 2 extractions covering ≥ 2 subcategories. For example, “Dosing route” splits each molecule’s LD50 measurements into {oral, injection, inhalation, dermal, ...} and asks how much of that molecule’s lethal-dose variance falls between routes (vs. within a route): $\eta^2 = 0.56$ means that over half of the variance for a single molecule’s LD50 measurements in the literature is explained by route, not noise. Definitions for groups are in Appendix D; all η^2 values significant with $p < 0.001$

Nuanced contexts are common and predictive, yet current datasets fail to capture them.

Starling data shows that differing experimental outcomes for the same molecule are meaningful, not just noise. We find such cases are common: for one-third of molecules with more than five Starling extractions in BBB and LD50, at least two distinct outcomes appear, each in at least 20% of extractions. Existing datasets would mislabel these molecules because they only consider structure.

Such context strongly affects label distributions across many tasks and is not noise. In Fig. 2, we use ANOVA to quantify it’s importance. The conditioning variables are from structured context, arising from interaction between sub-agents during extraction (e.g., dosing route, food state, sex, assay class, disease state, age group) and are output alongside the target values (e.g., binary labels

for Oral and BBB, and $\log_{10}(\text{mol/kg})$ for LD50)². For each (task, conditioning variable) pair we restrict to molecules with ≥ 2 extractions covering ≥ 2 subcategories of that variable and compute the fraction of total label variance explained by each conditioning variable (η^2). All structured nuance fields proposed by Starling are statistically significant and together explain a substantial proportion of variance in the observed labels. This supports the hypothesis that such context strongly influences measurements, and that assigning each molecule a single binary label, as current datasets do, discards systematically predictable biological behavior not captured by structure alone.

Nuanced contexts enable better characterization of model failures and improved training.

Much of the context we discover has known causal relationships with target properties but is entirely discarded by other resources. This makes it difficult to know when predictors trained on such data will succeed. In Table 5, using Starling contextual data for the BBB and LD50 tasks, we analyze MiniMol classifiers trained on the corresponding TDC datasets, stratified by contextual variables and evaluated on held-out Starling data. In BBB, molecules cross the blood-brain barrier mainly via passive diffusion, determined by physicochemical properties, and active influx via transporters such as Pgp. Table 5 highlights the issue: TDC data poorly covers Active influx molecules, and performance on this set is at chance. Starling more uniformly covers the main diffusion mechanisms, so training on our data yields a classifier that excels at all mechanisms (+Lit). A similar argument applies to LD50, where TDC poorly covers molecules that are more toxic by injection than by oral consumption.

Table 5: Stratified AUROC on held-out literature test sets. (a) BBB permeability grouped by each molecule’s dominant transport mechanism from the Starling-extracted `bbb_transport_label`: Passive (passive diffusion), Active influx (protein-mediated transport into the brain), and Efflux limited (active pumping out of the brain). (b) Rat oral LD50 grouped by the difference between oral and injection LD50 where available. In both panels, the eval target matches TDC’s. In both tasks, structure-only training fails in buckets where labels are most decoupled from structure; adding the literature corpus closes most of this gap, with negligible change in structurally typical buckets.

(a) BBB by transport mechanism				(b) Rat oral LD50 by oral-vs-injection Δ			
Mechanism	# Mols	TDC-only	+ Lit.	Oral vs Injection LD50	# Mols	TDC-only	+ Lit.
Passive diffusion	1949	0.665	0.728	Injection \approx Oral	386	0.836	0.842
Active influx	1207	0.443	0.693	Injection $>$ Oral	383	0.778	0.781
Efflux limited	897	0.573	0.727	Injection \gg Oral	384	0.557	0.706

7 Related Work

Scientific research agents. A growing class of LLM agents reads scientific literature to answer questions or execute workflows. PaperQA2 [55] is a representative narrative-answer system, retrieving and reranking passages to produce cited prose; Aviary [42] extends this with a gym and training framework for FutureHouse’s scientific agents, including a PaperQA-style literature environment. BioMNI [18] coordinates about 150 specialist tools and 59 biomedical databases to run research workflows, using the literature mainly for tool discovery rather than as a primary data source. In chemistry, ChemCrow [11] pairs an LLM with tools for synthesis planning, retrosynthesis, and literature search, while Coscientist [10] connects an LLM to wet-lab automation hardware to design and run experiments. AI Scientist V1 and V2 [32, 64] autonomously run machine-learning experiments and write papers. However, none sweep a corpus and emit *structured records at literature scale*.

LLM-based structured extraction from scientific text. Recent work applies LLMs to extract structured records from primary literature. Agrawal et al. [2] demonstrate few-shot clinical extraction; Dagdelen et al. [13] fine-tune GPT-3 to emit JSON records for materials chemistry, pursuing essentially the same goal as ours but at roughly four orders of magnitude smaller scale and with hand-crafted schemas for each task. Ai et al. [3] fine-tune a 7B model on 100K USPTO procedures to populate the Open Reaction Database schema with high accuracy.

Biomedical entity tagging. Existing NER taggers like PubTator3 [62] and BERN2 [56] support only fixed biomedical entity types via specialized models. Recent work shows that LLMs now match

²For this analysis, we manually filtered Starling’s discovered fields for those that vary within molecule. For example, we did not include “mechanism of action” because this nearly never varies within molecule and therefore cannot possibly explain variance in single-molecule measurements.

or surpass BERT-style taggers on biomedical NER [46], and UniversalNER [67] introduces the teacher–student distillation paradigm we adopt at literature scale.

8 Conclusion

Manually curated biomedical databases have long underpinned therapeutic AI, but are costly to build, lag behind the literature, and discard experimental context. As models advance, these limitations is becoming a hard ceiling. We show that primary literature can instead be autonomously converted into structured datasets, cheaply and at scale. Across six therapeutic-discovery tasks, Starling produces ~ 6.3 M records, yielding datasets that match or exceed the size and accuracy of the curated benchmarks they extend. The supporting passages and structured fields preserve key nuances—food state, dosing route, mechanism, assay class, disease state—that explain much of the within-molecule variance usually treated as noise. We release the datasets, code, and an API endpoint for our system.

References

- [1] OpenAI Sandhini Agarwal, Lama Ahmad, Jason Ai, Sam Altman, Andy Applebaum, Edwin Arbus, Rahul K. Arora, Yu Bai, Bowen Baker, Hai-Biao Bao, Boaz Barak, Ally Bennett, Tyler Bertao, N. Archer Brett, Eugene Brevdo, Greg Brockman, Sébastien Bubeck, Cheng Chang, Kai Chen, Mark Chen, Enoch Cheung, Aidan Clark, Dan Cook, Marat Dukhan, C. Dvorak, K Fives, Vlad Fomenko, T. Garipov, Kristian Georgiev, Mia Glaese, Tarun Gogineni, A. B. Goucher, Lukas Gross, Katia Gil Guzman, John Hallman, Jackie Hehir, Johannes Heidecke, Alec Helyar, Haitang Hu, Romain Huet, Jacob Huh, Saachi Jain, Zach Johnson, Chris Koch, Irina Kofman, Dominika Kundel, Jason Kwon, Volodymyr Kyrylov, Elaine Ya Le, Guillaume Leclerc, James Lennon, Scott Lessans, Mario Lezcano-Casado, Yuanzhi Li, Zhuohan Li, Ji Lin, Jordan Liss, Lily Liu, Jiancheng Liu, Kevin Lu, Chris Lu, Zoran N. Martinovic, Lindsay McCallum, Josh McGrath, Scott McKinney, Aidan McLaughlin, Song Mei, Steve Mostovoy, Tong Mu, Gideon Myles, Alexander Neitz, Alex Nichol, Jakub W. Pachocki, Alex Paino, Dana Palmie, Ashley Pantuliano, Giambattista Parascandolo, Jongsoo Park, Leher Pathak, Carolina Paz, Ludovic Peran, Dmitry Pimenov, Michelle Pocrass, Elizabeth Proehl, Huida Qiu, Gaby Raila, Filippo Raso, Hongyu Ren, K. Richardson, David Robinson, Bob Rotsted, Hadi Salman, Suvansh Sanjeev, Max Schwarzer, Daniel Sculley, Harshit S. Sikchi, Kendal Simon, Karan Singhal, Yang Song, Dane Stuckey, Zhiqing Sun, Phil Tillet, Sam Toizer, Foivos Tsimpourlas, Nikhil Vyas, Eric Wallace, Xin Wang, Miles Wang, Olivia Watkins, Kevin Weil, Amy E. Wendling, Kevin Whinnery, Cedric Whitney, Hannah Wong, Lin Yang, Yu Yang, Michihiro Yasunaga, Kristen Ying, Wojciech Zaremba, Wenting Zhan, Cyril Zhang, Brian Hu Zhang, Eddie Zhang, and Shengjia Zhao. gpt-oss-120b&gpt-oss-20b model card. 2025. URL <https://api.semanticscholar.org/CorpusID:280671456>.
- [2] Monica Agrawal, Stefan Hegselmann, Hunter Lang, Yoon Kim, and David Sontag. Large language models are few-shot clinical information extractors. In Yoav Goldberg, Zornitsa Kozareva, and Yue Zhang, editors, *Proceedings of the 2022 Conference on Empirical Methods in Natural Language Processing*, pages 1998–2022, Abu Dhabi, United Arab Emirates, December 2022. Association for Computational Linguistics. doi: 10.18653/v1/2022.emnlp-main.130. URL <https://aclanthology.org/2022.emnlp-main.130/>.
- [3] Qianxiang Ai, Fanwang Meng, Jiale Shi, Brenden Pelkie, and Connor W. Coley. Extracting structured data from organic synthesis procedures using a fine-tuned large language model. *Digital Discovery*, 3(9):1822–1831, September 2024. ISSN 2635-098X. doi: 10.1039/D4DD00091A. URL <https://pubs.rsc.org/en/content/articlelanding/2024/dd/d4dd00091a>.
- [4] Rolf Apweiler, Amos Bairoch, Cathy H. Wu, Winona C. Barker, Brigitte Boeckmann, Serenella Ferro, Elisabeth Gasteiger, Hongzhan Huang, Rodrigo Lopez, Michele Magrane, Maria J. Martin, Darren A. Natale, Claire O’Donovan, Nicole Redaschi, and Lai-Su L. Yeh. UniProt: the Universal Protein knowledgebase. *Nucleic Acids Research*, 32(Database issue):D115–D119, January 2004. ISSN 0305-1048. doi: 10.1093/nar/gkh131. URL <https://pmc.ncbi.nlm.nih.gov/articles/PMC308865/>.
- [5] Michael Ashburner, Catherine A. Ball, Judith A. Blake, David Botstein, Heather Butler, J. Michael Cherry, Allan P. Davis, Kara Dolinski, Selina S. Dwight, Janan T. Eppig, Midori A. Harris, David P. Hill, Laurie Issel-Tarver, Andrew Kasarskis, Suzanna Lewis, John C. Matese,

- Joel E. Richardson, Martin Ringwald, Gerald M. Rubin, and Gavin Sherlock. Gene Ontology: tool for the unification of biology. *Nature genetics*, 25(1):25–29, May 2000. ISSN 1061-4036. doi: 10.1038/75556. URL <https://pmc.ncbi.nlm.nih.gov/articles/PMC3037419/>.
- [6] Parit Bansal, Anne Morgat, Kristian B. Axelsen, Venkatesh Muthukrishnan, Elisabeth Coudert, Lucila Aimo, Nevila Hyka-Nouspikel, Elisabeth Gasteiger, Arnaud Kerhornou, Teresa Batista Neto, Monica Pozzato, Marie-Claude Blatter, Alex Ignatchenko, Nicole Redaschi, and Alan Bridge. Rhea, the reaction knowledgebase in 2022. *Nucleic Acids Research*, 50(D1):D693–D700, 2022. doi: 10.1093/nar/gkab1016. URL <https://doi.org/10.1093/nar/gkab1016>.
- [7] SM Bell, J Phillips, A Sedykh, A Tandon, C Sprinkle, SQ Morefield, A Shapiro, D Allen, R Shah, EA Maull, WM Casey, and NC Kleinstreuer. An integrated chemical environment to support 21st-century toxicology. *Environmental Health Perspectives*, 125(5):054501, 2017. doi: 10.1289/EHP1759. URL <https://doi.org/10.1289/EHP1759>.
- [8] Janos X. Binder, Sune Pletscher-Frankild, Kalliopi Tsafou, Christian Stolte, Sean I. O’Donoghue, Reinhard Schneider, and Lars Juhl Jensen. Compartments: unification and visualization of protein subcellular localization evidence. *Database*, 2014:bau012, 2014. doi: 10.1093/database/bau012. URL <https://doi.org/10.1093/database/bau012>.
- [9] Olivier Bodenreider. The Unified Medical Language System (UMLS): integrating biomedical terminology. *Nucleic Acids Research*, 32(Database issue):D267–D270, January 2004. ISSN 0305-1048. doi: 10.1093/nar/gkh061. URL <https://pmc.ncbi.nlm.nih.gov/articles/PMC308795/>.
- [10] Daniil A. Boiko, Robert MacKnight, Ben Kline, and Gabe Gomes. Autonomous chemical research with large language models. *Nature*, 624(7992):570–578, December 2023. ISSN 1476-4687. doi: 10.1038/s41586-023-06792-0. URL <https://www.nature.com/articles/s41586-023-06792-0>.
- [11] Andres M. Bran, Sam Cox, Oliver Schilter, Carlo Baldassari, Andrew D. White, and Philippe Schwaller. Augmenting large-language models with chemistry tools. *Nature Machine Intelligence*, 6(5):525–535, May 2024. doi: 10.1038/s42256-024-00832-8. URL <https://www.nature.com/articles/s42256-024-00832-8>.
- [12] Garth R. Brown, Vichet Hem, Kenneth S. Katz, Michael Ovetsky, Craig Wallin, Olga Ermolaeva, Igor Tolstoy, Tatiana Tatusova, Kim D. Pruitt, Donna R. Maglott, and Terence D. Murphy. Gene: a gene-centered information resource at NCBI. *Nucleic Acids Research*, 43(Database issue):D36–D42, January 2015. ISSN 0305-1048. doi: 10.1093/nar/gku1055. URL <https://pmc.ncbi.nlm.nih.gov/articles/PMC4383897/>.
- [13] John Dagdelen, Alexander Dunn, Sanghoon Lee, Nicholas Walker, Andrew S. Rosen, Gerbrand Ceder, Kristin A. Persson, and Anubhav Jain. Structured information extraction from scientific text with large language models. *Nature Communications*, 15(1):1418, February 2024. ISSN 2041-1723. doi: 10.1038/s41467-024-45563-x. URL <https://www.nature.com/articles/s41467-024-45563-x>.
- [14] Allan Peter Davis, Thomas C. Wieggers, Robin J. Johnson, Daniela Sciaky, Jolene Wieggers, and Carolyn J. Mattingly. Comparative toxicogenomics database (CTD): update 2023. *Nucleic Acids Research*, 51(D1):D1257–D1262, 2023. doi: 10.1093/nar/gkac833. URL <https://doi.org/10.1093/nar/gkac833>.
- [15] Kirill Degtyarenko, Paula de Matos, Marcus Ennis, Janna Hastings, Martin Zbinden, Alan McNaught, Rafael Alcántara, Michael Darsow, Mickaël Guedj, and Michael Ashburner. ChEBI: a database and ontology for chemical entities of biological interest. *Nucleic Acids Research*, 36 (Database issue):D344–D350, January 2008. ISSN 0305-1048. doi: 10.1093/nar/gkm791. URL <https://pmc.ncbi.nlm.nih.gov/articles/PMC2238832/>.
- [16] Tingjun Hou, Junmei Wang, Wei Zhang, and Xiaojie Xu. ADME evaluation in drug discovery. 6. Can oral bioavailability in humans be effectively predicted by simple molecular property-based rules? *Journal of Chemical Information and Modeling*, 47(2):460–463, 2007. doi: 10.1021/ci6003515.

- [17] Kexin Huang, Tianfan Fu, Wenhao Gao, Yue Zhao, Yusuf Roohani, Jure Leskovec, Connor W. Coley, Cao Xiao, Jimeng Sun, and Marinka Zitnik. Artificial intelligence foundation for therapeutic science. *Nature Chemical Biology*, 18:1033–1036, 2022. doi: 10.1038/s41589-022-01131-2. URL <https://doi.org/10.1038/s41589-022-01131-2>.
- [18] Kexin Huang, Serena Zhang, Hanchen Wang, Yuanhao Qu, Yingzhou Lu, Yusuf Roohani, Ryan Li, Lin Qiu, Junze Zhang, Yin Di, et al. Biomni: A general-purpose biomedical ai agent. *bioRxiv preprint*, 2025. doi: 10.1101/2025.05.30.656746.
- [19] Rachael P. Huntley, Tony Sawford, Prudence Mutowo-Meullenet, Aleksandra Shypitsyna, Carlos Bonilla, Maria J. Martin, and Claire O’Donovan. The GOA database: Gene Ontology annotation updates for 2015. *Nucleic Acids Research*, 43(Database issue):D1057–D1063, 2015. doi: 10.1093/nar/gku1113.
- [20] Alistair E. W. Johnson, Lucas Bulgarelli, Lu Shen, Alvin Gayles, Ayad Shammout, Steven Horng, Tom J. Pollard, Benjamin Moody, Brian Gow, Li wei H. Lehman, Leo Anthony Celi, and Roger G. Mark. Mimic-iv, a freely accessible electronic health record dataset. *Scientific Data*, 10, 2023. URL <https://doi.org/10.1038/s41597-022-01899-x>.
- [21] John M. Jumper, Richard Evans, Alexander Pritzel, Tim Green, Michael Figurnov, Olaf Ronneberger, Kathryn Tunyasuvunakool, Russ Bates, Augustin Žídek, Anna Potapenko, Alex Bridgland, Clemens Meyer, Simon A A Kohl, Andy Ballard, Andrew Cowie, Bernardino Romera-Paredes, Stanislav Nikolov, Rishub Jain, Jonas Adler, Trevor Back, Stig Petersen, David Reiman, Ellen Clancy, Michal Zielinski, Martin Steinegger, Michalina Pacholska, Tamas Berghammer, Sebastian Bodenstern, David Silver, Oriol Vinyals, Andrew W. Senior, Koray Kavukcuoglu, Pushmeet Kohli, and Demis Hassabis. Highly accurate protein structure prediction with alphafold. *Nature*, 596:583 – 589, 2021. URL <https://doi.org/10.1038/s41586-021-03819-2>.
- [22] Steven M. Kearnes, Michael R. Maser, Michael Wleklinski, Anton Kast, Abigail G. Doyle, Spencer D. Dreher, Joel M. Hawkins, Klavs F. Jensen, and Connor W. Coley. The Open Reaction Database. *Journal of the American Chemical Society*, 143(45):18820–18826, November 2021. ISSN 0002-7863. doi: 10.1021/jacs.1c09820. URL <https://doi.org/10.1021/jacs.1c09820>.
- [23] Marlene T. Kim, Alexander Sedykh, Suman K. Chakravarti, Roustem D. Saiakhov, and Hao Zhu. Critical evaluation of human oral bioavailability for pharmaceutical drugs by using various cheminformatics approaches, 2014.
- [24] Sunghwan Kim, Paul A. Thiessen, Evan E. Bolton, Jie Chen, Gang Fu, Asta Gindulyte, Lianyi Han, Jane He, Siqian He, Benjamin A. Shoemaker, Jiyao Wang, Bo Yu, Jian Zhang, and Stephen H. Bryant. PubChem Substance and Compound databases. *Nucleic Acids Research*, 44 (D1):D1202–1213, January 2016. ISSN 1362-4962. doi: 10.1093/nar/gkv951.
- [25] Kerstin Kläser, Błażej Banaszewski, Samuel Maddrell-Mander, Callum McLean, Luis Müller, Ali Parviz, Shenyang Huang, and Andrew Fitzgibbon. $\text{\texttt{MiniMol}}$: A Parameter-Efficient Foundation Model for Molecular Learning, April 2024. URL <http://arxiv.org/abs/2404.14986>. arXiv:2404.14986 [cs].
- [26] Craig Knox, Mike Wilson, Christen M Klinger, Mark Franklin, Eponine Oler, Alex Wilson, Allison Pon, Jordan Cox, Na Eun (Lucy) Chin, Seth A Strawbridge, Marysol Garcia-Patino, Ray Kruger, Aadhavaya Sivakumaran, Selena Sanford, Rahil Doshi, Nitya Khetarpal, Omolola Fatokun, Daphnee Doucet, Ashley Zubkowski, Dorsa Yahya Rayat, Hayley Jackson, Karxena Harford, Afia Anjum, Mahi Zakir, Fei Wang, Siyang Tian, Brian Lee, Jaanus Liigand, Harrison Peters, Ruo Qi (Rachel) Wang, Tue Nguyen, Denise So, Matthew Sharp, Rodolfo da Silva, Cyrella Gabriel, Joshua Scantlebury, Marissa Jasinski, David Ackerman, Timothy Jewison, Tanvir Sajed, Vasuk Gautam, and David S Wishart. DrugBank 6.0: the DrugBank Knowledgebase for 2024. *Nucleic Acids Research*, 52(D1):D1265–D1275, January 2024. ISSN 0305-1048. doi: 10.1093/nar/gkad976. URL <https://doi.org/10.1093/nar/gkad976>.
- [27] Melissa J. Landrum, Jennifer M. Lee, Mark Benson, Garth R. Brown, Chen Chao, Shanmuga Chitipiralla, Baoshan Gu, Jennifer Hart, Douglas Hoffman, Wonhee Jang, Karen Karapetyan,

- Kenneth Katz, Chunlei Liu, Zenith Maddipatla, Adriana Malheiro, Kurt McDaniel, Michael Ovetsky, George Riley, George Zhou, J. Bradley Holmes, Brandi L. Kattman, and Donna R. Maglott. ClinVar: improving access to variant interpretations and supporting evidence. *Nucleic Acids Research*, 46(D1):D1062–D1067, 2018. doi: 10.1093/nar/gkx1153. URL <https://doi.org/10.1093/nar/gkx1153>.
- [28] Jiawei Li, Minzhou Li, Qi Yang, and Sanzhong Luo. ReactionSeek: LLM-powered literature data mining and knowledge discovery in organic synthesis. *Nature Communications*, 17(1):3356, 2026. doi: 10.1038/s41467-026-70180-1. URL <https://www.nature.com/articles/s41467-026-70180-1>.
- [29] Yumeng Li, Guang Yang, Hao Liu, Bowen Wang, and Colin Zhang. dots.ocr: Multilingual document layout parsing in a single vision-language model, 2025. URL <https://arxiv.org/abs/2512.02498>.
- [30] Zhiyuan Liu, Yaorui Shi, An Zhang, Sihang Li, Enzhi Zhang, Xiang Wang, Kenji Kawaguchi, and Tat-Seng Chua. ReactXT: Understanding molecular “reaction-ship” via reaction-contextualized molecule-text pretraining. In Lun-Wei Ku, Andre Martins, and Vivek Srikumar, editors, *Findings of the Association for Computational Linguistics: ACL 2024*, pages 5353–5377, Bangkok, Thailand, August 2024. Association for Computational Linguistics. doi: 10.18653/v1/2024.findings-acl.318. URL <https://aclanthology.org/2024.findings-acl.318/>.
- [31] Daniel M. Lowe, Peter T. Corbett, Peter Murray-Rust, and Robert C. Glen. Chemical Name to Structure: OPSIN, an Open Source Solution. *Journal of Chemical Information and Modeling*, 51(3):739–753, March 2011. ISSN 1549-9596. doi: 10.1021/ci100384d. URL <https://doi.org/10.1021/ci100384d>.
- [32] Chris Lu, Cong Lu, Robert Tjarko Lange, Jakob Foerster, Jeff Clune, and David Ha. The AI Scientist: Towards Fully Automated Open-Ended Scientific Discovery, September 2024. URL <http://arxiv.org/abs/2408.06292>. arXiv:2408.06292 [cs].
- [33] Jiang Lu, Lianlian Wu, Ruijiang Li, Mengxuan Wan, Jun Yang, Peng Zan, Hui Bai, Song He, and Xiaochen Bo. Toxacol: an endpoint-aware and task-focused compound representation learning paradigm for acute toxicity assessment. *Nature Communications*, 16:5992, 2025. doi: 10.1038/s41467-025-60989-7. URL <https://doi.org/10.1038/s41467-025-60989-7>.
- [34] Jakub Lála, Odhran O’Donoghue, Aleksandar Shtedritski, Sam Cox, Samuel G. Rodrigues, and Andrew D. White. PaperQA: Retrieval-Augmented Generative Agent for Scientific Research, December 2023. URL <http://arxiv.org/abs/2312.07559>. arXiv:2312.07559 [cs].
- [35] Chang-Ying Ma, Sheng-Yong Yang, Hui Zhang, Mingli Xiang, Qi Huang, and Yuquan Wei. Prediction models of human plasma protein binding rate and oral bioavailability derived by using ga-cg-svm method. *Journal of Pharmaceutical and Biomedical Analysis*, 47(4–5):677–682, 2008. doi: 10.1016/j.jpba.2008.03.023. URL <https://doi.org/10.1016/j.jpba.2008.03.023>.
- [36] Iyad Majid, Vaibhav Mishra, Rohith Ravindranath, and Sophia Y. Wang. Evaluating the Performance of Large Language Models for Named Entity Recognition in Ophthalmology Clinical Free-Text Notes. *AMIA Annual Symposium Proceedings*, 2024:778–787, May 2025. ISSN 1942-597X. URL <https://pmc.ncbi.nlm.nih.gov/articles/PMC12099357/>.
- [37] Kamel Mansouri, Agnes L. Karmaus, Jeremy Fitzpatrick, Grace Patlewicz, Prachi Pradeep, Domenico Alberga, Nathalie Alepee, Timothy E. H. Allen, Dave Allen, Vinicius M. Alves, Carolina H. Andrade, Tyler R. Auernhammer, Davide Ballabio, Shannon Bell, Emilio Benfenati, Sudin Bhattacharya, Joyce V. Bastos, Stephen Boyd, J. B. Brown, Stephen J. Capuzzi, Yaroslav Chushak, Heather Ciallella, Alex M. Clark, Viviana Consonni, Pankaj R. Daga, Sean Ekins, Sherif Farag, Maxim Fedorov, Denis Fourches, Domenico Gadaleta, Feng Gao, Jeffery M. Gearhart, Garrett Goh, Jonathan M. Goodman, Francesca Grisoni, Christopher M. Grulke, Thomas Hartung, Matthew Hirn, Pavel Karpov, Alexandru Korotcov, Giovanna J. Lavado, Michael Lawless, Xinhao Li, Thomas Luechtefeld, Filippo Lunghini, Giuseppe F. Mangiatordi, Gilles Marcou, Dan Marsh, Todd Martin, Andrea Mauri, Eugene N. Muratov, Glenn J. Myatt, Duc-Trung Nguyen, Orazio Nicolotti, Reine Note, Paritosh Pande, Amanda K. Parks, Tyler

- Peryea, Ahsan H. Polash, Robert Rallo, Alessandra Roncaglioni, Craig Rowlands, Patricia Ruiz, Daniel P. Russo, Ahmed Sayed, Risa Sayre, Timothy Sheils, Charles Siegel, Arthur C. Silva, Anton Simeonov, Sergey Sosnin, Noel Southall, Judy Strickland, Yun Tang, Brian Teppen, Igor V. Tetko, Dennis Thomas, Valery Tkachenko, Roberto Todeschini, Cosimo Toma, Ignacio Tripodi, Daniela Trisciuzzi, Alexander Tropsha, Alexandre Varnek, Kristijan Vukovic, Zhongyu Wang, Ligu Wang, Katrina M. Waters, Andrew J. Wedlake, Sanjeeva J. Wijeyesakere, Dan Wilson, Zijun Xiao, Hongbin Yang, Gergely Zahoranszky-Kohalmi, Alexey V. Zakharov, Fagen F. Zhang, Zhen Zhang, Tongan Zhao, Hao Zhu, Kimberley M. Zorn, Warren Casey, and Nicole C. Kleinstreuer. CATMoS: Collaborative acute toxicity modeling suite. *Environmental Health Perspectives*, 129(4):047013, 2021. doi: 10.1289/EHP8495. URL <https://doi.org/10.1289/EHP8495>.
- [38] Antonio Rueda Martin, Eleanor Williams, Rebecca E. Foulger, Sarah Leigh, Louise C. Daugherty, Olivia Niblock, Ivone U. S. Leong, Katherine R. Smith, Oleg Gerasimenko, Eik Haraldsdottir, Ellen Thomas, Richard H. Scott, Emma Baple, Arianna Tucci, Helen Brittain, Anna de Burca, Kristina Ibañez, Dalia Kasperaviciute, Damian Smedley, Mark Caulfield, Augusto Rendon, and Ellen M. McDonagh. PanelApp crowdsources expert knowledge to establish consensus diagnostic gene panels. *Nature Genetics*, 51(11):1560–1565, 2019. doi: 10.1038/s41588-019-0528-2.
- [39] Ines Filipa Martins, Ana L. Teixeira, Luis Pinheiro, and Andre O. Falcao. A bayesian approach to in silico blood-brain barrier penetration modeling. *Journal of Chemical Information and Modeling*, 52(6):1686–1697, 2012. doi: 10.1021/ci300124c. URL <https://doi.org/10.1021/ci300124c>.
- [40] Fanwang Meng, Yang Xi, Jinfeng Huang, and Paul W. Ayers. A curated diverse molecular database of blood-brain barrier permeability with chemical descriptors. *Scientific Data*, 8(1):289, October 2021. ISSN 2052-4463. doi: 10.1038/s41597-021-01069-5. URL <https://www.nature.com/articles/s41597-021-01069-5>.
- [41] Ludovico Mitchener, Angela Yiu, Benjamin Chang, Mathieu Bourdenx, Tyler Nadolski, Arvis Sulovari, Eric C. Landsness, Dániel L. Barabási, Siddharth Narayanan, Nicky Evans, Shriya Reddy, Martha S. Foiani, Aizad Kamal, Leah P. Shriver, Fang Cao, Asmamaw T. Wassie, Jon M. Laurent, Edwin Melville-Green, Mayk Caldas Ramos, Albert Bou, Kaleigh F. Roberts, Sladjana Zagorac, Timothy C. Orr, Miranda E. Orr, Kevin J. Zvezdaryk, Ali E. Ghareeb, Laurie McCoy, Bruna Gomes, Euan A Ashley, Karen E. Duff, Tonio Buonassisi, Tom Rainforth, Randall J. Bateman, Michael Skarlinski, Samuel G. Rodrigues, Michaela M. Hinks, and Andrew D. White. Kosmos: An ai scientist for autonomous discovery. *ArXiv*, abs/2511.02824, 2025. URL <https://api.semanticscholar.org/CorpusID:282748827>.
- [42] Siddharth Narayanan, James D. Braza, Ryan-Rhys Griffiths, Manu Ponnappati, Albert Bou, Jon Laurent, Ori Kabeli, Geemi Wellawatte, Sam Cox, Samuel G. Rodrigues, and Andrew D. White. Aviary: training language agents on challenging scientific tasks, December 2024. URL <http://arxiv.org/abs/2412.21154>. arXiv:2412.21154 [cs].
- [43] National Center for Biotechnology Information. Generif: Gene reference into function. <https://www.ncbi.nlm.nih.gov/gene/about-generif>.
- [44] Mark Neumann, Daniel King, Iz Beltagy, and Waleed Ammar. ScispaCy: Fast and robust models for biomedical natural language processing. In Dina Demner-Fushman, Kevin Bretonnel Cohen, Sophia Ananiadou, and Junichi Tsujii, editors, *Proceedings of the 18th BioNLP Workshop and Shared Task*, pages 319–327, Florence, Italy, August 2019. Association for Computational Linguistics. doi: 10.18653/v1/W19-5034. URL <https://aclanthology.org/W19-5034/>.
- [45] Zhangming Niu, Xianglu Xiao, Wenfan Wu, Qiwei Cai, Yinghui Jiang, Wangzhen Jin, Minhao Wang, Guojian Yang, Linggang Kong, Xurui Jin, Guang Yang, and Hongming Chen. Pharmabench: Enhancing admet benchmarks with large language models. *Scientific Data*, 11(1):985, 2024. doi: 10.1038/s41597-024-03793-0. URL <https://doi.org/10.1038/s41597-024-03793-0>.
- [46] Motasem S Obeidat, Md Sultan Al Nahian, and Ramakanth Kavuluru. Do LLMs Surpass Encoders for Biomedical NER? *Proceedings. IEEE International Conference on Healthcare Informatics*, 2025:352–358, June 2025. ISSN 2575-2626. doi: 10.1109/ICHI64645.2025.00048. URL <https://pmc.ncbi.nlm.nih.gov/articles/PMC12335919/>.

- [47] Guillaume Ollitrault, Marco Marzo, Alessandra Roncaglioni, Emilio Benfenati, Olivier Taboureau, and Enrico Mombelli. Qsar models for predicting oral bioavailability and volume of distribution and their application in mapping the tk space of endocrine disruptors. *Journal of Xenobiotics*, 15(5):166, 2025. doi: 10.3390/jox15050166. URL <https://doi.org/10.3390/jox15050166>.
- [48] Lukas Minus Orre, Mattias Vesterlund, Yanbo Pan, Taner Arslan, Yafeng Zhu, Alejandro Fernandez Woodbridge, Oliver Frings, Erik Fredlund, and Janne Lehtiö. SubCellBarCode: Proteome-wide mapping of protein localization and relocalization. *Molecular Cell*, 73(1): 166–182.e7, 2019. doi: 10.1016/j.molcel.2018.11.035.
- [49] Janet Piñero, Juan Manuel Ramírez-Anguita, Josep Saüch-Pitarch, Francesco Ronzano, Emilio Centeno, Ferran Sanz, and Laura I. Furlong. The DisGeNET knowledge platform for disease genomics: 2019 update. *Nucleic Acids Research*, 48(D1):D845–D855, 2020. doi: 10.1093/nar/gkz1021.
- [50] Sune Pletscher-Frankild, Albert Pallegà, Kalliopi Tsafou, Janos X. Binder, and Lars Juhl Jensen. Diseases: Text mining and data integration of disease–gene associations. *Methods*, 74:83–89, 2015. doi: 10.1016/j.ymeth.2014.11.020. URL <https://doi.org/10.1016/j.ymeth.2014.11.020>.
- [51] Victor Sabanza Gil, Andres M. Bran, Malte Franke, Rémi Schlama, Jeremy S. Luterbacher, and Philippe Schwaller. Holistic chemical evaluation reveals pitfalls in reaction prediction models. In *NeurIPS 2023 AI for Science Workshop*, 2023. doi: 10.48550/arXiv.2312.09004. URL <https://arxiv.org/abs/2312.09004>.
- [52] Conrad L Schoch, Stacy Ciufu, Mikhail Domrachev, Carol L Hotton, Sivakumar Kannan, Rogneda Khovanskaya, Detlef Leipe, Richard Mcveigh, Kathleen O’Neill, Barbara Robbertse, Shobha Sharma, Vladimir Soussov, John P Sullivan, Lu Sun, Seán Turner, and Ilene Karsch-Mizrachi. NCBI Taxonomy: a comprehensive update on curation, resources and tools. *Database: The Journal of Biological Databases and Curation*, 2020:baaa062, August 2020. ISSN 1758-0463. doi: 10.1093/database/baaa062. URL <https://pmc.ncbi.nlm.nih.gov/articles/PMC7408187/>.
- [53] Zhihong Shao, Peiyi Wang, Qihao Zhu, Runxin Xu, Junxiao Song, Xiao Bi, Haowei Zhang, Mingchuan Zhang, Y. K. Li, Y. Wu, and Daya Guo. DeepSeekMath: Pushing the Limits of Mathematical Reasoning in Open Language Models, February 2024. URL <https://arxiv.org/abs/2402.03300v3>.
- [54] Aaditya Singh, Adam Fry, Adam Perelman, Adam Tart, Adi Ganesh, Ahmed El-Kishky, Aidan McLaughlin, Aiden Low, A. J. Ostrow, Akhila Ananthram, Akshay Nathan, Alan Luo, Alec Helyar, Aleksander Madry, Aleksandr Efremov, Aleksandra Spyra, Alex Baker-Whitcomb, Alex Beutel, Alex Karpenko, Alex Makelov, Alex Neitz, Alex Wei, Alexandra Barr, Alexandre Kirchmeyer, Alexey Ivanov, Alexi Christakis, Alistair Gillespie, Allison Tam, Ally Bennett, Alvin Wan, Alyssa Huang, Amy McDonald Sandjideh, Amy Yang, Ananya Kumar, Andre Saraiva, Andrea Vallone, Andrei Gheorghe, Andres Garcia Garcia, Andrew Braunstein, Andrew Liu, Andrew Schmidt, Andrey Mereskin, Andrey Mishchenko, Andy Applebaum, Andy Rogerson, Ann Rajan, Annie Wei, Anoop Kotha, Anubha Srivastava, Anushree Agrawal, Arun Vijayvergiya, Ashley Tyra, Ashvin Nair, Avi Nayak, Ben Eggers, Bessie Ji, Beth Hoover, Bill Chen, Blair Chen, Boaz Barak, Borys Minaiev, Botao Hao, Bowen Baker, Brad Lightcap, Brandon McKinzie, Brandon Wang, Brendan Quinn, Brian Fioca, Brian Hsu, Brian Yang, Brian Yu, Brian Zhang, Brittany Brenner, Callie Riggins Zetino, Cameron Raymond, Camillo Lugaresi, Carolina Paz, Cary Hudson, Cedric Whitney, Chak Li, Charles Chen, Charlotte Cole, Chelsea Voss, Chen Ding, Chen Shen, Chengdu Huang, Chris Colby, Chris Hallacy, Chris Koch, Chris Lu, Christina Kaplan, Christina Kim, C. J. Minott-Henriques, Cliff Frey, Cody Yu, Coley Czarnecki, Colin Reid, Colin Wei, Cory Decareaux, Cristina Scheau, Cyril Zhang, Cyrus Forbes, Da Tang, Dakota Goldberg, Dan Roberts, Dana Palmie, Daniel Kappler, Daniel Levine, Daniel Wright, Dave Leo, David Lin, David Robinson, Declan Grabb, Derek Chen, Derek Lim, Derek Salama, Dibya Bhattacharjee, Dimitris Tsipras, Dinghua Li, Dingli Yu, D. J. Strouse, Drew Williams, Dylan Hunn, Ed Bayes, Edwin Arbus, Ekin Akyurek, Elaine Ya Le, Elana Widmann, Eli Yani, Elizabeth Proehl, Enis Sert, Enoch Cheung, Eri Schwartz, Eric Han,

Eric Jiang, Eric Mitchell, Eric Sigler, Eric Wallace, Erik Ritter, Erin Kavanaugh, Evan Mays, Evgenii Nikishin, Fangyuan Li, Felipe Petroski Such, Filipe de Avila Belbute Peres, Filippo Raso, Florent Bekerman, Foivos Tsimpourlas, Fotis Chantzis, Francis Song, Francis Zhang, Gaby Raila, Garrett McGrath, Gary Briggs, Gary Yang, Giambattista Parascandolo, Gildas Chabot, Grace Kim, Grace Zhao, Gregory Valiant, Guillaume Leclerc, Hadi Salman, Hanson Wang, Hao Sheng, Haoming Jiang, Haoyu Wang, Haozhun Jin, Harshit Sikchi, Heather Schmidt, Henry Aspegren, Honglin Chen, Huida Qiu, Hunter Lightman, Ian Covert, Ian Kivlichan, Ian Silber, Ian Sohl, Ibrahim Hammoud, Ignasi Clavera, Ikai Lan, Ilge Akkaya, Ilya Kostrikov, Irina Kofman, Isak Etinger, Ishaan Singal, Jackie Hehir, Jacob Huh, Jacqueline Pan, Jake Wilczynski, Jakub Pachocki, James Lee, James Quinn, Jamie Kiros, Janvi Kalra, Jasmyn Samaroo, Jason Wang, Jason Wolfe, Jay Chen, Jay Wang, Jean Harb, Jeffrey Han, Jeffrey Wang, Jennifer Zhao, Jeremy Chen, Jerene Yang, Jerry Tworek, Jesse Chand, Jessica Landon, Jessica Liang, Ji Lin, Jiancheng Liu, Jianfeng Wang, Jie Tang, Jihan Yin, Joanne Jang, Joel Morris, Joey Flynn, Johannes Ferstad, Johannes Heidecke, John Fishbein, John Hallman, Jonah Grant, Jonathan Chien, Jonathan Gordon, Jongsoo Park, Jordan Liss, Jos Kraaijeveld, Joseph Guay, Joseph Mo, Josh Lawson, Josh McGrath, Joshua Vendrow, Joy Jiao, Julian Lee, Julie Steele, Julie Wang, Junhua Mao, Kai Chen, Kai Hayashi, Kai Xiao, Kamyar Salahi, Kan Wu, Karan Sekhri, Karan Sharma, Karan Singhal, Karen Li, Kenny Nguyen, Keren Gu-Lemberg, Kevin King, Kevin Liu, Kevin Stone, Kevin Yu, Kristen Ying, Kristian Georgiev, Kristie Lim, Kushal Tirumala, Kyle Miller, Lama Ahmad, Larry Lv, Laura Clare, Laurance Fauconnet, Lauren Itow, Lauren Yang, Laurentia Romaniuk, Leah Anise, Lee Byron, Leher Pathak, Leon Maksin, Leyan Lo, Leyton Ho, Li Jing, Liang Wu, Liang Xiong, Lien Mamitsuka, Lin Yang, Lindsay McCallum, Lindsey Held, Liz Bourgeois, Logan Engstrom, Lorenz Kuhn, Louis Feuvrier, Lu Zhang, Lucas Switzer, Lukas Kondraciuk, Lukasz Kaiser, Manas Joglekar, Mandeep Singh, Mandip Shah, Manuka Stratta, Marcus Williams, Mark Chen, Mark Sun, Marselus Cayton, Martin Li, Marvin Zhang, Marwan Aljubeih, Matt Nichols, Matthew Haines, Max Schwarzer, Mayank Gupta, Meghan Shah, Melody Huang, Meng Dong, Mengqing Wang, Mia Glaese, Micah Carroll, Michael Lampe, Michael Malek, Michael Sharman, Michael Zhang, Michele Wang, Michelle Pokrass, Mihai Florian, Mikhail Pavlov, Miles Wang, Ming Chen, Mingxuan Wang, Minnia Feng, Mo Bavarian, Molly Lin, Moose Abdool, Mostafa Rohaninejad, Nacho Soto, Natalie Staudacher, Natan LaFontaine, Nathan Marwell, Nelson Liu, Nick Preston, Nick Turley, Nicklas Ansmann, Nicole Blades, Nikil Pancha, Nikita Mikhaylin, Niko Felix, Nikunj Handa, Nishant Rai, Nitish Keskar, Noam Brown, Ofir Nachum, Oleg Boiko, Oleg Murk, Olivia Watkins, Oona Gleeson, Pamela Mishkin, Patryk Lesiewicz, Paul Baltescu, Pavel Belov, Peter Zhokhov, Philip Pronin, Phillip Guo, Phoebe Thacker, Qi Liu, Qiming Yuan, Qinghua Liu, Rachel Dias, Rachel Puckett, Rahul Arora, Ravi Teja Mullapudi, Raz Gaon, Reah Miyara, Rennie Song, Rishabh Aggarwal, R. J. Marsan, Robel Yemiru, Robert Xiong, Rohan Kshirsagar, Rohan Nuttall, Roman Tsiupa, Ronen Eldan, Rose Wang, Roshan James, Roy Ziv, Rui Shu, Ruslan Nigmatullin, Saachi Jain, Saam Talaie, Sam Altman, Sam Arnesen, Sam Toizer, Sam Toyer, Samuel Miserendino, Sandhini Agarwal, Sarah Yoo, Savannah Heon, Scott Ethersmith, Sean Grove, Sean Taylor, Sebastien Bubeck, Sever Banesiu, Shaokyi Amdo, Shengjia Zhao, Sherwin Wu, Shibani Santurkar, Shiyu Zhao, Shraman Ray Chaudhuri, Shreyas Krishnaswamy, Shuaiqi Xia, Shuyang Cheng, Shyamal Anadkat, Simón Posada Fishman, Simon Tobin, Siyuan Fu, Somay Jain, Song Mei, Sonya Egoian, Spencer Kim, Spug Golden, S. Q. Mah, Steph Lin, Stephen Imm, Steve Sharpe, Steve Yadlowsky, Sulman Choudhry, Sungwon Eum, Suvansh Sanjeev, Tabarak Khan, Tal Stramer, Tao Wang, Tao Xin, Tarun Gogineni, Taya Christianson, Ted Sanders, Tejal Patwardhan, Thomas Degry, Thomas Shadwell, Tianfu Fu, Tianshi Gao, Timur Garipov, Tina Sriskandarajah, Toki Sherbakov, Tomer Kaftan, Tomo Hiratsuka, Tongzhou Wang, Tony Song, Tony Zhao, Troy Peterson, Val Kharitonov, Victoria Chernova, Vineet Kosaraju, Vishal Kuo, Vitchyr Pong, Vivek Verma, Vlad Petrov, Wanning Jiang, Weixing Zhang, Wenda Zhou, Wenlei Xie, Wenting Zhan, Wes McCabe, Will DePue, Will Ellsworth, Wulfie Bain, Wyatt Thompson, Xiangning Chen, Xiangyu Qi, Xin Xiang, Xinwei Shi, Yann Dubois, Yaodong Yu, Yara Khakbaz, Yifan Wu, Yilei Qian, Yin Tat Lee, Yinbo Chen, Yizhen Zhang, Yizhong Xiong, Yonglong Tian, Young Cha, Yu Bai, Yu Yang, Yuan Yuan, Yuanzhi Li, Yufeng Zhang, Yuguang Yang, Yujia Jin, Yun Jiang, Yunyun Wang, Yushi Wang, Yutian Liu, Zach Stubenvoll, Zehao Dou, Zheng Wu, and Zhigang Wang. OpenAI GPT-5 System Card, December 2025. URL <http://arxiv.org/abs/2601.03267>. arXiv:2601.03267 [cs].

- [55] Michael D. Skarlinski, Sam Cox, Jon M. Laurent, James D. Braza, Michaela Hinks, Michael J. Hammerling, Manvitha Ponnampati, Samuel G. Rodrigues, and Andrew D. White. Language agents achieve superhuman synthesis of scientific knowledge, September 2024. URL <http://arxiv.org/abs/2409.13740>. arXiv:2409.13740 [cs].
- [56] Mujeen Sung, Minbyul Jeong, Yonghwa Choi, Donghyeon Kim, Jinhyuk Lee, and Jaewoo Kang. BERN2: an advanced neural biomedical named entity recognition and normalization tool. *Bioinformatics*, 38(20):4837–4839, October 2022. ISSN 1367-4811. doi: 10.1093/bioinformatics/btac598. URL <https://doi.org/10.1093/bioinformatics/btac598>.
- [57] Tongyi DeepResearch Team, Baixuan Li, Bo Zhang, Dingchu Zhang, Fei Huang, Guangyu Li, Guoxin Chen, Hui Feng Yin, Jialong Wu, Jingren Zhou, Kuan Li, Liangcai Su, Litu Ou, Liwen Zhang, Pengjun Xie, Rui Ye, Wenbiao Yin, Xinmiao Yu, Xinyu Wang, Xixi Wu, Xuanzhong Chen, Yida Zhao, Zhen Zhang, Zhengwei Tao, Zhongwang Zhang, Zile Qiao, Chenxi Wang, Donglei Yu, Gang Fu, Haiyang Shen, Jiayin Yang, Jun Lin, Junkai Zhang, Kui Zeng, Li Yang, Hailong Yin, Maojia Song, Ming Yan, Minpeng Liao, Peng Xia, Qian Xiao, Rui Min, Ruixue Ding, Runnan Fang, Shaowei Chen, Shen Huang, Shihang Wang, Shihao Cai, Weizhou Shen, Xiaobin Wang, Xin Guan, Xinyu Geng, Yingcheng Shi, Yuning Wu, Zhuo Chen, Zijian Li, and Yong Jiang. Tongyi DeepResearch Technical Report, October 2025. URL <https://arxiv.org/abs/2510.24701v2>.
- [58] Peter J. Thul, Lovisa Åkesson, Mikaela Wiking, Diana Mahdessian, Aikaterini Geladaki, Hammou Ait Blal, Tove Alm, Anna Asplund, Lars Björk, Lisa M. Breckels, Anna Bäckström, Frida Danielsson, Linn Fagerberg, Jenny Fall, Laurent Gatto, Christian Gnann, Sophia Hober, Martin Hjelmare, Fredric Johansson, Sunjae Lee, Cecilia Lindskog, Jan Mulder, Claire M. Mulvey, Peter Nilsson, Per Oksvold, Johan Rockberg, Rutger Schutten, Jochen M. Schwenk, Åsa Sivertsson, Evelina Sjöstedt, Marie Skogs, Charlotte Stadler, Devin P. Sullivan, Hanna Tegel, Casper Winsnes, Cheng Zhang, Martin Zwahlen, Adil Mardinoglu, Fredrik Pontén, Kalle von Feilitzen, Kathryn S. Lilley, Mathias Uhlén, and Emma Lundberg. A subcellular map of the human proteome. *Science*, 356(6340):eaal3321, 2017. doi: 10.1126/science.aal3321. URL <https://doi.org/10.1126/science.aal3321>.
- [59] Manthana V. S. Varma, R. Scott Obach, Charles Rotter, Howard R. Miller, George Chang, Stefanus J. Steyn, Ayman El-Kattan, and Matthew D. Troutman. Physicochemical space for optimum oral bioavailability: Contribution of human intestinal absorption and first-pass elimination. *Journal of Medicinal Chemistry*, 53(3):1098–1108, 2010. doi: 10.1021/jm901371v.
- [60] Jonathan T. Wall, Risa R. Sayre, Doris Smith, Samuel Winter, Maxwell Groover, Jasmine Hope, Adriana Webb, Katie Paul Friedman, Madison Feshuk, Antony J. Williams, Charles Lowe, Nisha S. Sipes, Jason Lambert, Jennifer H. Olker, Russell S. Thomas, Colleen Elonen, Richard S. Judson, and Chelsea A. Weitekamp. Development of the toxicity values database, toxvaldb: A curated resource for experimental and derived human health-relevant toxicity data. *Computational Toxicology*, 35:100365, 2025. doi: 10.1016/j.comtox.2025.100365. URL <https://doi.org/10.1016/j.comtox.2025.100365>.
- [61] Fangping Wan, Felix Wong, James J. Collins, and César de la Fuente-Nunez. Machine learning for antimicrobial peptide identification and design. *Nature Reviews Bioengineering*, 2:392–407, 2024. URL <https://doi.org/10.1038/s44222-024-00152-x>.
- [62] Chih-Hsuan Wei, Alexis Allot, Po-Ting Lai, Robert Leaman, Shubo Tian, Ling Luo, Qiao Jin, Zhizheng Wang, Qingyu Chen, and Zhiyong Lu. Pubtator 3.0: an AI-powered literature resource for unlocking biomedical knowledge. *Nucleic Acids Research*, 52(W1):W540–W546, 2024. doi: 10.1093/nar/gkae235. URL <https://doi.org/10.1093/nar/gkae235>.
- [63] Min Wei, Xudong Zhang, Xiaolin Pan, Bo Wang, Changge Ji, Yifei Qi, and John Z. H. Zhang. Hobpre: accurate prediction of human oral bioavailability for small molecules. *Journal of Cheminformatics*, 14(1), 2022. doi: 10.1186/s13321-021-00580-6. URL <https://doi.org/10.1186/s13321-021-00580-6>.
- [64] Yutaro Yamada, Robert Tjarko Lange, Cong Lu, Shengran Hu, Chris Lu, Jakob Foerster, Jeff Clune, and David Ha. The AI Scientist-v2: Workshop-Level Automated Scientific Discovery via Agentic Tree Search, April 2025. URL <http://arxiv.org/abs/2504.08066>. arXiv:2504.08066 [cs].

- [65] Barbara Zdrazil, Eloy Felix, Fiona Hunter, Emma J. Manners, James Blackshaw, Sybilla Corbett, Marleen de Veij, Harris Ioannidis, David Mendez Lopez, Juan F. Mosquera, Maria Paula Magarinos, Nicolas Bosc, Ricardo Arcila, Tevfik Kizilören, Anna Gaulton, A. Patrícia Bento, Melissa F. Adasme, Peter Monecke, Gregory A. Landrum, and Andrew R. Leach. The ChEMBL database in 2023: a drug discovery platform spanning multiple bioactivity data types and time periods. *Nucleic Acids Research*, 52(D1):D1180–D1192, 2024. doi: 10.1093/nar/gkad1004. URL <https://doi.org/10.1093/nar/gkad1004>.
- [66] Yanzhao Zhang, Mingxin Li, Dingkun Long, Xin Zhang, Huan Lin, Baosong Yang, Pengjun Xie, An Yang, Dayiheng Liu, Junyang Lin, Fei Huang, and Jingren Zhou. Qwen3 Embedding: Advancing Text Embedding and Reranking Through Foundation Models, June 2025. URL <http://arxiv.org/abs/2506.05176>. arXiv:2506.05176 [cs].
- [67] Wenxuan Zhou, Sheng Zhang, Yu Gu, Muhao Chen, and Hoifung Poon. UniversalNER: Targeted Distillation from Large Language Models for Open Named Entity Recognition. *International Conference on Learning Representations*, 2024:12276–12294, May 2024. URL https://proceedings.iclr.cc/paper_files/paper/2024/hash/34678d08b36076de986df95c5bbba92f-Abstract-Conference.html.
- [68] Hao Zhu, Todd M. Martin, Lin Ye, Alexander Sedykh, Douglas M. Young, and Alexander Tropsha. Quantitative structure–activity relationship modeling of rat acute toxicity by oral exposure. *Chemical Research in Toxicology*, 22(12):1913–1921, 2009. doi: 10.1021/tx900189p. URL <https://doi.org/10.1021/tx900189p>.

A Release Plan, Limitations, and Broader Impact

A core goal of this work is to make self-driving dataset construction broadly available to the research community. Two constraints make a single, monolithic release impractical:

Licensing. Our 22.5M-paper corpus is assembled under journal- and publisher-specific licensing terms that permit our internal use of the full text for AI workloads but do not extend to redistribution. We cannot release the corpus or the per-paper extracted text. We are not yet sure whether we can release the dense embeddings derived from it. Re-extracting, running OCR, and processing an equivalent corpus is possible for any institution with the appropriate licenses, but it is not a casual undertaking.

Engineering. The production version of Starling is built on top of retrieval and indexing infrastructure designed specifically for fast querying over 250M chunks and 4.5B entity mentions: sharded ClickHouse bitmap indexes for entity filters, Milvus for dense vector search, custom fusion-scoring code, and ingestion pipelines for keeping the indexes consistent across re-tagging passes. Most of this complexity exists because the underlying corpus is enormous; it would be nearly all dead weight on a corpus of, say, 10K papers, and releasing it as-is would saddle adopters with infrastructure they neither need nor can usefully replicate without the corpus it was built around.

We therefore adopt a two-pronged release strategy designed to give different audiences the right level of access while respecting both constraints.

A.1 Hosted Access to the Full System

The first prong preserves access to Starling *as deployed*—running over the full 22.5M-paper corpus, with all of its tagging, normalization, and retrieval infrastructure intact. We plan to release this as an MCP (Model Context Protocol) server that exposes Starling’s full end-to-end extraction pipeline to the client. Crucially, the server performs no LLM inference of its own: all model calls are issued back to the client as MCP sampling requests, which the client fulfills using its own LLM endpoint (whether a hosted API, an internal deployment, or local compute). The client pays for its own inference; we pay only for the database queries. Researchers can then use whichever LLMs they prefer, including frontier models that would be cost-prohibitive for us to serve at corpus scale.

We commit to maintaining this hosted access as long as serving costs remain tractable, which we think should be possible as the plan detailed above only requires us to serve a CPU-only database, not LLM endpoints. If aggregate query load grows beyond what we can absorb, we will introduce

per-account rate limits before restricting access; the goal is to keep the system available to academic users.

A.2 Self-Hostable Open-Source Release

The second prong is a fully open-source version of *Starling* that any institution can stand up on a corpus they have rights to. This release ships the same agent definitions, prompts, schema-induction logic, filter-design loops, validators, and extractors used in the hosted system—the recipes are identical—so that results obtained on a self-hosted corpus are directly comparable in methodology to those obtained against ours.

We will abstract the retrieval tools to be able to run with any database backend, both the somewhat complex mixture of systems we chose for scale and simpler to stand up ones like DuckDB plus FAISS. We provide reference implementations for both small and large corpora. The API contract guarantees that *Starling* itself will run unchanged against any backend that satisfies it.

We also release the entity tagger model weights and the schemas, prompts, and configuration files for each of the six tasks reported in the main paper, so that a self-hosted deployment can reproduce our extractions on the user’s own corpus, and so that practitioners can use them as templates for new extraction tasks.

A.3 Limitations and Broader Impact

Starling reads text and tables but not figures, so any property reported only in a plot is currently unavailable to the agent. Accessing this data will require a multimodal extractor. Our corpus is licensed for internal use, but not for redistribution, so external groups can reproduce the methodology, but without our forthcoming API endpoint or an independent license to the same corpus, they cannot reproduce our exact results. In terms of extraction quality, they inherit the biases and errors that may be found in scientific literature, and inherit the errors that may arise when using LLMs at scale. Care was taken to minimize the errors that make it out of our pipeline, with an error rate ranging from 0.6 to 7.78% per task.

Data provenance. *Starling* has no opinions about data provenance or how to weight evidence or data from different papers or sources. The extraction agent takes the claims made in papers at face value. While it is therefore possible to build an understanding of the landscape for particular molecules, genes, or reactions (for example), *Starling*-collected data does not meet the stringent evidentiary standard of collections like ClinVar.

Dual-use. *Starling* lowers the cost and latency of building literature-grounded biomedical datasets, which we expect to make therapeutic AI work that has historically required well-funded curation efforts accessible to academic groups and smaller labs. Several of our case studies (notably LD50 and Ora1) carry mild dual-use potential: the same records that accelerate therapeutic design also lower the cost of toxicity-aware harmful design. This dual-use concern is typical of AI for science systems, but is nevertheless always worth flagging.

Necessary judging. Another issue worth flagging here is the need for judging. The first pass extraction run results in many potentially lower quality extractions, and we used GPT-5.4 and distillation to effectively and cheaply combat this. The use of *Starling* without effective judging could easily create a flood of low quality data given the low cost of running *Starling*. In ongoing work, we hope to bake judging directly into the extraction process to more completely eliminate this potential pitfall.

A.4 Summary

To summarize, the following are released openly:

- The *Starling* agent system, including all agent definitions, prompts, and orchestration code.
- The fine-tuned entity tagger model weights, along with the per-category prompts and few-shot examples used to train it.
- Reference implementations of the retrieval backend at two scales.
- Task specifications, induced schemas, and configuration files for all six datasets reported in the main paper.

- The six datasets themselves, including extracted records and the verbatim supporting passages whose excerpts fall within fair-use bounds.
- An MCP server providing hosted access to Starling running over the full PubMed corpus.

The following are *not* released, and cannot be released under our current licensing terms:

- The 22.5M-paper corpus itself, including extracted text, markdown conversions, and dense embeddings.
- The production retrieval infrastructure, which is tightly coupled to internal data layouts and would not be useful to external users in isolation.

We believe this combination—hosted access to the production system plus a self-hostable open-source equivalent—makes the methodology of this paper reproducible and extensible by the research community, while honoring the licensing terms under which we obtained access to the underlying literature.

B Deep Research Agent Baselines

We evaluate five frontier AI systems on their ability to perform open-ended biomedical data extraction from PubMed. Each system was given the same five prompts, with no constraints on methodology. The goal is to assess whether current “deep research” agents can autonomously produce structured, validated, PubMed-traceable scientific datasets.

B.1 Task Descriptions

Each model received the same prompt per task, mirroring the original prompts to Starling, with minor variations for models that support CSV download requests. The five prompts are shown in Figure 3.

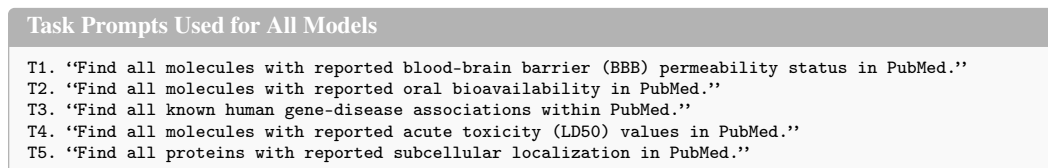


Figure 3: The five natural-language task prompts given to each model. Minor wording variations were used only for models that supported explicit CSV download requests.

B.2 Experimental Setup

Models evaluated. We compare five agent configurations spanning different architectures and tool-use modalities:

1. **BioMNI-Phylo:** A sandboxed Python coding agent with iterative cell execution, access to tools such as NCBI E-utilities, ChEMBL, PubChem APIs, and NLP libraries (scispaCy). Produces execution trace notebooks alongside output CSVs.
2. **Claude Research Mode** (Opus 4.6 Extended): A web-based deep research agent on claude.ai that produces comprehensive narrative reports. As it cannot produce data files, we pair it with a *continuation agent* (Claude Code) that executes the recommended pipelines to produce CSVs. This constitutes a two-stage pipeline.
3. **GPT-5.4 Deep Research:** A web-based deep research agent on chatgpt.com that produces comprehensive narrative reports. Like Claude Research Mode, it produces no data files; a continuation agent executes the designed pipelines. This is the only configuration that attempted genuine PubMed text mining (E-utilities + PubTator + regex extraction) for 4 of 5 tasks.
4. **GPT-5.4 Pro Extended Thinking:** OpenAI ChatGPT’s code interpreter / tool-use mode, prompted to return a downloadable CSV. This agent autonomously produced complete CSVs for 4 of 5 tasks in a single session by identifying and reformatting pre-existing databases.
5. **Kosmos AI-Scientist** (Edison Scientific): An autonomous research agent that runs a multi-step discovery loop — hypothesis generation, code execution against curated databases and PubMed, iterative refinement, and report writing — and ships per-task “master” CSVs alongside a discovery PDF and bundled intermediate artefacts. Of the five baselines, Kosmos is the only one that

performs explicit self-curation steps within its own pipeline (e.g., a redistributed-benchmark detector that flags PMC5494643, the Jain 2024 NCI/CADD QSAR file, and excludes it from the LD50 master), but it does not apply a per-row LLM judge to the published master. Like GPT-5.4 Pro, Kosmos produces final CSVs autonomously without a continuation agent.

Producing usable artifacts. GPT-5.4 Pro received a “return a downloadable CSV” suffix and produced data files directly; Kosmos AI-Scientist received the bare task prompt because its discovery loop ships CSVs natively. Claude Research Mode and GPT-5.4 Deep Research produced narrative reports rather than data files regardless of CSV-request phrasing, so for those two we executed the report’s recommended pipeline with a local continuation agent (Claude Code, Opus 4.6, 1M-context) that downloaded the cited databases or APIs and normalized and merged them into the final CSV file.

Strategies employed. The baseline agents generally adopted one of the following strategies:

1. **Download (DL):** The agent found instances primarily by downloading pre-existing databases (e.g., B3DB for BBB, PubTator3/BioREx bulk files for GDA).
2. **Download and Aggregate (DLA):** The agent aggregated multiple pre-existing databases to form a larger database.
3. **Literature extraction (LE):** The agent performed genuine, original text mining from scientific articles.
4. **Hybrid (H):** The agent employed some hybrid of the first three strategies in the sample pipeline (e.g., BioMNI-Phylo on T1/T2/T4, Kosmos on T4/T5).

We annotate the strategies taken by each agent on each task in Table 6.

Table 6: Strategies adopted by the deep research system across the various tasks. Notable crossovers: GPT-5.4 Deep Research’s T3 (loaded the pre-computed PubTator3/BioREx bulk file rather than fresh NLP → S1), BioMNI-Phylo’s T3 and T5 (dropped the API layer entirely → S3), and Kosmos AI-Scientist’s T4/T5 (S2 backbone augmented with PubMed/PMC-OA full-text mining → H).

Agent	T1 BBB	T2 Oral	T3 GDA	T4 LD50	T5 PSL
BioMNI-Phylo	H	H	LE	H	LE
Claude Research	DLA	DLA	DLA	DLA	DLA
GPT-5.4 Deep Res.	LE	LE	DL	LE	LE
GPT-5.4 Pro	DL	DL	DL	DL	DL
Kosmos AI-Sci.	DLA	DLA	DLA	H	H

B.3 Results

Table 7 presents aggregate dataset statistics for the collections gathered by the baseline agents across all 25 (model × task) evaluations. We organize by task and report output scale, identifier quality, PubMed traceability, and estimated data validity for each model. We note here that, because deep research systems were generally not designed for this task, the datasets collected are not without some caveats that we explore in appendix B.4.

Validation methodology. We audited each of the 25 (5 models × 5 tasks) outputs using automated validation scripts and manual spot-checks. Validation dimensions: row counts, identifier validity (SMILES via RDKit, UniProt/gene symbols against canonical lists), and PMID resolvability. Where an agent dropped recoverable per-row PMIDs during its own deduplication, we restore them on the agent’s behalf using upstream dataset provenance (see Footnotes ^b and ^q of Table 7); this is a deliberately permissive choice that credits each baseline at the dataset level rather than penalizing it for losing provenance during post-processing.

B.4 Notes on Table 7

What rows do we keep for each agent? None of the five baselines applies a per-row quality audit; rows are emitted as-is by the chosen pipeline (database download, multi-DB union, or one-shot text mining). Starling, by contrast, runs the production judge from Section 3.2; the headline numbers we report are post-filter. To make the comparison conservative *against* Starling, we credit every baseline row at face value in Table 7, and where an agent dropped recoverable PMIDs during its own deduplication we restore them on the agent’s behalf (^b, ^q, see “Rescued PMIDs” below). Nevertheless,

Table 7: Comprehensive results for 5 models \times 5 tasks. **Rows**: total output rows. **Unique**: deduplicated entities (molecules, genes, or proteins). **ID Fill**: fraction of rows with structural identifiers (SMILES for molecular tasks, UniProt/gene symbols for others). **ID Valid**: fraction of filled identifiers that pass validation. **PMID Fill**: fraction of rows with ≥ 1 PubMed ID (counts dataset-aggregator PMIDs at face value; ^b, ^q are values we recovered on the agent’s behalf when it dropped upstream PMIDs during dedup). **Valid**: agent-reported fraction of well-formed rows (no per-row LLM audit applied to baselines; the contrast with Starling’s filtered output is discussed in §B.4).

Model	Rows	Unique Entities	ID Fill	ID Valid	PMID Fill	Valid
T1 – Blood-Brain Barrier Permeability						
BioMNI-Phylo	8,741	8,741	100%	99.9%	91.8%	~100%
Claude Research	20,177	8,716	100%	100%	$\geq 38.7\%^b$	~100%
GPT-5.4 Deep Res.	11,004	6,463	54.6%	100%	100%	~100%
GPT-5.4 Pro	7,796	7,796	100%	99.97%	0.18%	~100%
Kosmos AI-Sci.	9,955	9,955	100%	100%	$\geq 88.5\%^q$	~99%
T2 – Oral Bioavailability						
BioMNI-Phylo	14,089	12,763	90.6%	100%	99.0%	~96%
Claude Research	4,525	2,007	100%	100%	100%	~97%
GPT-5.4 Deep Res.	823	553	68.8%	100%	100%	~99%
GPT-5.4 Pro	995	995	100%	100%	0%	~99%
Kosmos AI-Sci.	32,609	22,707	100%	100%	93.8%	~99%
T3 – Gene-Disease Associations						
BioMNI-Phylo	74,018	8,065	100%	98.1%	100%	~84%
Claude Research	38.4M	28,514	100%	100%	99.0%	0.92%
GPT-5.4 Deep Res.	1.45M	23,899	100%	100%	100%	>99%
GPT-5.4 Pro	10,961	5,097	100%	100%	0%	~99%
Kosmos AI-Sci.	4.13M	26,939	100%	100%	96.1%	>99%
T4 – Acute Toxicity (LD50)						
BioMNI-Phylo	15,542	8,975	48.9%	100%	0.26%	~93%
Claude Research	186,827	90,373	71.7%	100%	0%	~99%
GPT-5.4 Deep Res.	1,132	871	50.4%	100%	100%	~92%
GPT-5.4 Pro	8,507	8,507	0%	—	0%	~99%
Kosmos AI-Sci.	162,531	99,633	96.0%	100%	34.9%	~99%
T5 – Protein Subcellular Localization						
BioMNI-Phylo	14,016	14,016	32.8%	99.1%	100%	~97%
Claude Research	369,273	362,143	98.1%	>99%	14.4%	~99%
GPT-5.4 Deep Res.	1,226	1,147	49.4%	>99%	100%	94–96%
GPT-5.4 Pro	580,017	78,981	96.4%	100%	0%	~98%
Kosmos AI-Sci.	529,268	19,907	100%	100%	34.1%	~99%

Markers ^{b,q} refer to PMID rescues we performed on the agent’s behalf; see §B.4.

Table 8: Primary data sources used by each agent on each task. Rows of Table 7 reference these sources; "PubMed mining" indicates original literature extraction (E-utilities + PubTator + regex).

Task	BioMNI-Phylo	Claude Research	GPT-5.4 Deep Res.	GPT-5.4 Pro	Kosmos AI-Sci.
T1 BBB	B3DB, BBBP, PubTator NER [40, 39, 62]	B3DB, PharmaBench, TDC, BBBP [40, 45, 17, 39]	PubMed mining	B3DB [40]	B3DB, ChEMBL, PubChem [40, 65, 24]
T2 Oral	ChEMBL, PubMed NLP [65]	HobPre, Kim, TDC, QSAR-TK [63, 23, 35, 47]	PubMed mining	Kim et al. 2014 [23]	ChEMBL, HobPre, Hou, Varma [65, 63, 16, 59]
T3 GDA	PubMed co-mention NLP	CTD, DISEASES, ClinVar, GeneRIF [14, 50, 27, 43]	PubTator3 (BioREx) [62]	NCBI ClinVar [27]	PubTator3, DisGeNET, CTD, PanelApp [62, 49, 14, 38]
T4 LD50	PubChem HSDB, ChEMBL, PubMed mining [24, 65]	NCI/CADD, ToxValDB, CATMoS, TDC [33, 60, 37, 68]	PubMed mining	NICEATM/ICE [7]	PubChem ChemIDplus, ChEMBL, PubMed mining [24, 65]
T5 PSL	PubMed, scispaCy NER, NCBI Gene [44]	UniProt, HPA, GO, COMPARTMENTS [4, 58, 5, 8]	PubMed mining	COMPARTMENTS (7 sp.) [8]	GOA, UniProt, PMC-OA mining, COMPARTMENTS, HPA, SubCellBarCode [19, 4, 8, 58, 48]

we *do* only count rows where (1) a valid normalizable entity was recoverable, and (2) a valid label was given. For example for (1), for small molecule property tasks, we discard rows where we could not recover a valid SMILES string or name that we could normalize to a SMILES string. For example for (2), we discard rows that an agent extracted with `bbb_status=unknown` or similar.

Downloading datasets. On most (agent, task) cells the baseline downloads one or two curated source databases and reshapes them: BBB agents pull B3DB / BBBP / PharmaBench; Oral agents pull ChEMBL plus HobPre / Hou / Varma / Kim. The full per-cell source attribution is in Table 8. The substantive work of deciding which (entity, label) pairs are real and which papers warrant them was done upstream by the human curators, not the agent. Per-row data integrity is good across the cohort, but we do note that downloading a dataset is not directly comparable to collecting one *de novo* from the literature.

Claimed per-row literature sometimes doesn't hold up. We found that, in many baseline cases with high PMID fill, the citations were dataset-aggregator references rather than per-row primary literature (e.g., 4 distinct PMIDs across Claude Research's 4,525 T2 Oral rows).

Rescued PMIDs. For two cells in Table 7 (^b Claude Research T1 BBB, ^a Kosmos T1 BBB), the agent dropped recoverable upstream PMIDs during its own deduplication; we restore dataset-level PMIDs on the agent's behalf via the preserved source-database tags, lifting both cells from 0% to non-trivial PMID fill.

C Case Study: Large-Scale Reaction Extraction from PubMed

We apply `Starling` to chemical reaction mining across the full PubMed corpus, producing structured reaction records (products, reactants, catalysts, solvents, yields, conditions) from over 2M papers in a single automated run. The agent produced 163 probes covering 630 unique entity-name strings, further expanded at query time via the entity-normalization hierarchy (Section 2.1). Each prompt instructs the model to extract structured reaction records using the 12-field schema in Table 11 under “Ours”, designed to capture the full characterization of a chemical reaction.

C.1 Results

Statistics for the final dataset collected by `Starling` are detailed in Table 9.

Table 9: Statistics for the `Starling` reactions dataset.

Metric	Judge-filtered
Total reaction records	916,948
Unique PMIDs	259,679
Unique products	507,957
Unique reactions (reactant–product)	806,584
Novel products (not in 5-ref union)	401,055 (79.0%)

Reference datasets. We evaluate our extractions against five established reaction and compound databases (ORD [22], CHORISO [51], OpenExp [30], Rhea [6], ReactionSeek [28]); their domains, sizes, and the resolved-product counts we use for downstream coverage analysis are summarized in Table 10.

Coverage. For reactions, we define coverage as the fraction of a reference dataset’s unique canonical product SMILES that appear in our extraction set: $\text{Cov}(R) = |S_{\text{ours}} \cap S_R| / |S_R|$, where S_{ours} is our set of resolved product SMILES and S_R is the reference set. This measures how much of the known reaction product space our extraction recovers, independent of precision.

The variation in coverage across datasets reflects fundamental differences in source domain rather than extraction quality.

- **Rhea** (10.1%) has the highest coverage because it is the only dataset with systematic PubMed linkage (18.7K PMIDs). Our PubMed-sourced corpus naturally overlaps with Rhea’s biochemical literature.
- **CHORISO** (4.9%) represents academic journal chemistry. Despite no direct paper linkage, we rediscover a substantial fraction of its 1.9M products through canonical-SMILES matching, indicating substantial overlap between PubMed and the high-impact chemistry literature in CHORISO’s upstream CJHIF set.
- **ORD** (1.6%) is predominantly patent-derived (74.5% USPTO). Since PubMed indexes journal articles rather than patents, low overlap is expected.

Reaction novelty and scale comparison. Of the 507,957 unique resolved products in the judge-filtered release, 401,055 (79.0%) are *novel*—not present in any of the five reference datasets (3,479,157 combined unique products after deduplication). The reference-only products are predominantly patent chemistry (ORD 74.5% patents, OpenExp fully patent-derived), a domain where PubMed has inherently minimal overlap. We compare scale at the level of unique (reactant, product) pairs (canonical-SMILES signatures): the judge-filtered release contains 806,584 such pairs against $\sim 1.58\text{M}$ for ORD, giving $\sim 0.51 \times$ ORD (cf. Table 1, main paper). By the same axis we are $\sim 3.1 \times$ OpenExp and $\sim 82 \times$ Rhea, our only reference with systematic PubMed linkage.

C.2 Schema Richness vs. Reference Reaction Databases

Coverage tells us *which* reactions our extraction recovers, but not *what we know about each one*. Headline-scale tables equate ORD, CHORISO, and Rhea with our extraction, though they are structurally far simpler. Our 12-field schema, populated at 23–100% per field on the judge-filtered release, captures conditions and nuances that these reference datasets sometimes or often discard.

Table 10: Reference datasets used for evaluation. “Raw” is the dataset size as originally reported; “Resolved” is the number of unique canonical product SMILES after our RDKit canonicalization pipeline.

Dataset	Domain	Num. Reactions	Resolved Products	Source
ORD	Patents (74.5%)	2.4M	1,431,123	Kearnes et al. 2021
CHORISO	Academic journals	2.2M	1,905,747	Sabanza Gil et al. 2023
OpenExp	Patents (USPTO+ORD)	274K pairs	262,512	Liu et al. 2024
Rhea	Biochemistry (PubMed)	18.3K	9,869	Bansal et al. 2022
ReactionSeek	Org. Syntheses (LLM)	1,740 TP entries	635	Li et al. 2026
Combined (deduped)		—	3,479,157	

Table 11: Per-record fill rates of the structured schema columns each reaction database ships, plus per-record provenance/procedure rows. “—” means the field does not exist in the dataset’s released schema. “Ours” is the judge-filtered release (916,948 records). Reactants and product fields are universally populated and omitted; their structural form is documented in Section C.1.

Field	Starling (916K)	ORD (2.38M)	CHORISO (2.22M)	OpenExp (274K)	Rhea (18.3K)	RxnSeek (3.96K)
reaction_type	96%	—	—	—	—	—
reagent	60%	5%	90%	—	—	—
catalyst	23%	13%	5%	11%	—	—
solvent	61%	63%	83%	92%	—	89%
yield_percent	56%	44%	100% ^a	—	—	92%
yield_type	64%	—	—	—	—	—
outcome_status	100%	—	—	—	—	—
temperature	52%	21%	—	78%	—	91%
reaction_time	52%	42%	—	90%	—	91%
setup_and_notes	86%	—	—	—	—	—
support_text (paragraph-cited)	100%	—	—	100%	—	—
procedure_text (any granularity)	100%	75%	—	100%	—	100%
DOI/PMID linkage	100%	98%	—	—	95%	100%

^a CHORISO’s yield field is populated on every record, but $\sim 44\%$ of values are 0.0, indicating either failed reactions or missing data. Non-zero yield fills 55.7% of records.

Table 11 compares the conditions and provenance fields side by side—reactants and product, which all five reference datasets carry on essentially every record (in varying form: SMILES, ChEBI IDs, or IUPAC names per the breakdown in Section C.1), are omitted to focus on the schema-breadth gap. Fields marked “—” are schema fields that Starling chose but that are absent from the baseline dataset.

D Conditioning-variable Definitions for Fig. 2

Each plain-language label in Fig. 2 corresponds to a single field in the LLM-curated extraction schema. Below we list the field name (in parentheses) and the full set of subcategory values used to compute within-molecule η^2 . Records with null values for a given field are excluded from that row’s computation.

Oral bioavailability. **Age group** (developmental_stage) — fetal, neonatal, pediatric, adult. **CYP metabolizer phenotype** (metabolizer_capacity) — low (PM or CYP inhibitor), medium (EM), high (UM or CYP inducer). **Sex** — male, female, mixed. **Food state** (food_effect) — fasted, fed-standard, fed-high-fat, fed-low-fat, other. **Co-administered drug** (drug_interaction) — boolean: PK-affecting co-drug present (true) or absent (false). **Disease state** — none, hepatic impairment, renal impairment, diabetes, cancer, GI disease, other.

BBB. Permeability endpoint (metric_type) — absolute CNS concentration ($\mu\text{g/g}$ brain), brain:blood ratio (K_p), CSF:blood ratio, transfer permeability (PS, P_{app}), dose fraction (%ID/g), imaging radiotracer (PET / SPECT), other. **Species** — mouse, rat, human. **Assay class** (assay_type)

— ex-vivo tissue (post-mortem brain homogenate), fluid sampling (microdialysis or CSF tap), in-vivo imaging, BBB permeability assay (*in situ* perfusion, intracarotid upstream injection), behavioral / functional, *in silico*, other. **Brain disease state** (`bbb_disease`) — none, tumor, inflammation, ischemia (stroke), trauma (TBI), metabolic, neurodegenerative, other. **Age group** (`developmental_stage`) — fetal, neonatal, pediatric, adult. **Barrier integrity** (`bbb_integrity`) — intact, disrupted, severely disrupted.

LD50. Dosing route (`route`) — oral, injection-systemic (IV / IP / SC), injection-CNS (intracerebral or intrathecal), intramuscular, topical / dermal, inhalation, other. **Sex** — male, female, mixed. **Co-administered drug** (`co_treatment`) — boolean: another compound co-administered (true) or not (false). **Toxicity endpoint** (`assay_type`) — LD50 (median lethal dose), LC50 (median lethal concentration; inhalation), fatal-dose (any reported lethal dose).

E Selected “Clear” Errors from Human Evaluation of BBB_Martins

Here, we provide selected “obviously wrong” mislabelings that we identified in BBB_Martins during our human evaluation of BBB_Martins ↔ Starling disagreement.

Table 12: Existing manually curated datasets have errors that are not just in the tail. This table presents five drugs that have well known *canonical* labels for blood-brain barrier penetration but are mislabeled in the BBB_Martins dataset. Included is the literature consensus label as well as the fraction of extractions bearing that label.

Drug	TDC	Lit. consensus	n_{lit}	Mechanism / why TDC is wrong
Thiopental	BBB−	BBB+, rate 1.00	81	Canonical fast-acting IV anaesthetic with central GABA _A action. PMID 11270237, 23973449, 30147453
Levodopa	BBB−	BBB+, rate 0.91	2,503	Active LAT1 transport; first-line Parkinson’s drug. PMID 14683550, 17181137, 22434495
Propranolol	BBB−	BBB+, rate 0.98	1,169	CNS-penetrant β -blocker used for migraine and performance anxiety. PMID 20170117, 21605061, 30031971
Loperamide	BBB+	BBB−, rate 0.29	1,015	P-gp efflux substrate; net brain exposure is near-zero in intact BBB. PMID 18203948, 20162690, 21428839
Isoniazid	BBB−	BBB+, rate 0.96	390	First-line drug for tubercular meningitis precisely because it crosses. PMID 1803699, 23529866, 353023

F Starling Agent Details

This section covers the parts of the Starling pipeline that are most useful for reading the rest of the paper: the role of each agent, the rubric the Validator and Judge share, the probe-construction loop, how the retrieval set is ordered for extraction, how the production judge is trained, and the cost of an extraction run. Concrete artifacts are not reproduced here; they are included in the code release alongside the agent definitions and orchestration code.

F.1 Agent Roles

Starling coordinates five agents across query construction and extraction. Table 13 summarizes their inputs, outputs, and the model class each runs on.

Table 13: Agent inputs, outputs, and driving model. Qwen3.5-9B is distilled from GPT-5.4.

Agent	Input	Output	Model
Proposer	Task description; current probe set; Validator and Investigator feedback	New/revise probes (filter + semantic query); induced schema and task instantiation	GPT-5.4
Validator	Sampled passage or candidate extraction; rubric	Per-axis pass/fail and relevance verdict	gpt-oss-120b
Investigator	Validator-rejected passages; current filter	Natural-language refinement suggestions	gpt-oss-120b
Extractor	Retrieved window; schema; task instantiation	Structured record(s) with support passage	Gemma 4 31B
Judge	Extraction; support text; rubric	Per-axis pass/fail	Qwen3.5-9B

F.2 Judge Rubric

Every extraction is graded along five binary axes, only being admitted into the dataset if it fails on none of none of them. The same rubric is shared across all six tasks.

Support Fidelity. *Is the `support_text` a faithful rendering of the source evidence from the paper?*

Pass: the support text is well grounded in the paper, drawing from the cited paragraph or from nearby paragraphs, tables, or figures; light rewriting, paraphrasing, and reasonable conclusions from stated facts are fine as long as meaning and factual details remain faithful. Fail: the support text cannot be supported by the paper, materially distorts it, or fabricates details.

Task Relevance. *Does this extraction fall within the scope defined by the task?* Pass: the extraction captures exactly the type of data the task asks for. Fail: the extraction is clearly out of scope (for example, a general physiology statement or a different property entirely).

Molecule Attribution. *Is the named entity actually the subject of the claim in this support text?*

Pass: the entity is the subject of the extracted claim and is either explicitly named in the support text, unambiguously established by immediate surrounding context, or referred to by a recognized synonym (e.g., noradrenaline for norepinephrine, acetylsalicylic acid for aspirin). Fail: the entity is not the subject of the claim, or is absent from both the support text and its immediate context.

Label Correctness. *Is the primary label (the key outcome of the extraction) correct given the support text and its context?*

Pass: the primary outcome accurately reflects what the text states; the focus is on the headline label, not on auxiliary or descriptive fields. Fail: the primary label contradicts the text.

Accuracy. *Is the core factual claim of the extraction faithful to the source text?*

Pass: the primary claim is supported by the text and nothing contradicts the source. This dimension is about factual faithfulness, not about whether the best possible schema field was chosen for a given value. Fail: the extraction contradicts the source or fabricates information not stated or inferable from the paper.

F.3 Probe Loop and Schema Induction

The probe-construction loop in Section 3.1 terminates when the `Validator` estimates $\geq 80\%$ precision and a $\leq 15\%$ recall gap per probe, or when a configured probe-count cap is hit. The recall gap is estimated by sampling 50 papers that are highly ranked by at least one probe’s `semantic_query` but excluded by every probe’s entity filter, and asking the `Validator` what fraction carry relevant evidence. On the five non-Reactions tasks the loop converges to roughly 8 probes per task, with Reactions being an exception, running from 37 hand-authored task specifications that the loop expands into 163 probes.

Schema induction follows once the probe set is frozen. The `Proposer` samples 100 papers from the probe union and runs the `Extractor` on each in free-form mode (no fixed schema). The free-form records and the `Validator`’s per-axis scores on them are returned to the `Proposer`, which proposes a unified schema and a concrete *task instantiation*—the natural-language description of what counts as a valid record, what to ignore, and what default assumptions to use—and re-scores. In practice the schema fields stabilize after the first pass; almost all of the iteration is the `Proposer` sharpening the task instantiation so that the `Extractor` stops emitting boundary cases the `Validator` disagrees with.

F.4 Subcorpus Ranking

Once the probe set is frozen, the union of windows that match any probe forms the candidate subcorpus. The `Extractor` processes papers in priority order, ranking each paper by a weighted sum of three signals: (i) the number of probes whose entity filter the paper satisfies (probe-hit count), (ii) the mean semantic similarity between the paper’s windows and the probes’ semantic queries, and (iii) the maximum such similarity over the paper’s windows. The hit count rewards papers jointly relevant to multiple aspects of the task; the mean and max together favor papers that are either densely on-topic or contain a single highly-relevant passage.

F.5 Distilled Judge Training

The production judge from Section 3.2 is Qwen3.5-9B distilled from GPT-5.4 verdicts on the five-axis rubric above. Per task we collect 5,000 GPT-5.4-graded extractions (30,000 across the six tasks),

split 3,000 / 1,000 / 1,000 into SFT, GRPO, and held-out eval. SFT trains the judge to reproduce GPT-5.4’s per-axis pass/fail labels across all tasks and is refined with GRPO.

E.6 Extraction Cost Breakdown

The headline figure of \sim \$0.001 per kept record (Section 5.1) is dominated by `Extractor` inference. Planning, schema induction, and judge filtering combined are an order of magnitude smaller and amortized across all kept records for a task. Table 14 reports the per-task token volume and B200 GPU-hours for the extraction stage; in aggregate we run 42.3B input and 11.2B output tokens through the `Extractor`, totaling \sim 3,233 B200 GPU-hours.

Table 14: Extraction-stage inference volume per task.

Task	Input tokens	Output tokens	GPU-hours
Reactions	33.6B	5.80B	2,035
PSL	3.12B	2.06B	453
GDA	2.60B	2.03B	431
BBB	1.94B	792M	197
Oral	556M	252M	60.7
LD50	537M	233M	56.8
Total	42.3B	11.2B	3,233

The dollar cost of this volume varies by an order of magnitude across deployment paths. We benchmark three: a hosted-API call to the same model class through OpenRouter (\$0.13/M input tokens, \$0.38/M output tokens), a vLLM deployment on rented Vast.ai GPUs (\$3.85/GPU-hour), and a vLLM deployment on internal compute (\$1.00/GPU-hour). The corresponding total extraction costs across all six tasks are \$9,749, \$12,448, and \$3,233, respectively.

G Corpus Details

The full set of entity types tagged within our corpus are: Anatomy, Antibody, Assay/Result, CellLine, CellType, ClinicalTrial, Disease, Gene, GeneVariant, GOTerm, Organism, Pathway, Peptide, Phenotype, Protein, Protein/GeneFamily, RNA, SmallMolecule, and SmallMoleculeClass.

Section 2.2 introduces the entity filters that `Starling`’s sub-agents author; we give a concrete example here. The filter specification in Fig. 4 is one of the probes the `Proposer` constructed for the BBB task.

```
{
  "entity_groups": [
    ["SmallMolecule"],
    ["blood-brain barrier", "cerebrospinal fluid"]
  ],
  "semantic_query": "Reported blood-brain barrier (BBB) permeability or brain
penetration status for a named compound, including statements that the
compound crosses/penetrates or does not cross the BBB (permeable/impermeable),
or quantitative measures such as brain-to-plasma ratio (Kp), CSF concentration,
logBB, in situ brain perfusion, microdialysis, PAMPA-BBB/MDCK permeability used
as evidence of BBB penetration."
}
```

Figure 4: One of the `FilterSpec` probes the `Proposer` constructed for the BBB task. `entity_groups` is a CNF entity constraint (outer AND, inner OR); `semantic_query` is the rerank target applied to the surviving windows.

H Additional Results Measuring Disagreement for Individual Molecules

In this section, we present two small case studies that measure the variability of BBB, Oral and LD50 labels that exists for single molecules. Unlike existing resources for small molecule properties, `Starling` contains many extractions for some molecules. It’s reasonable to ask: how reasonable are

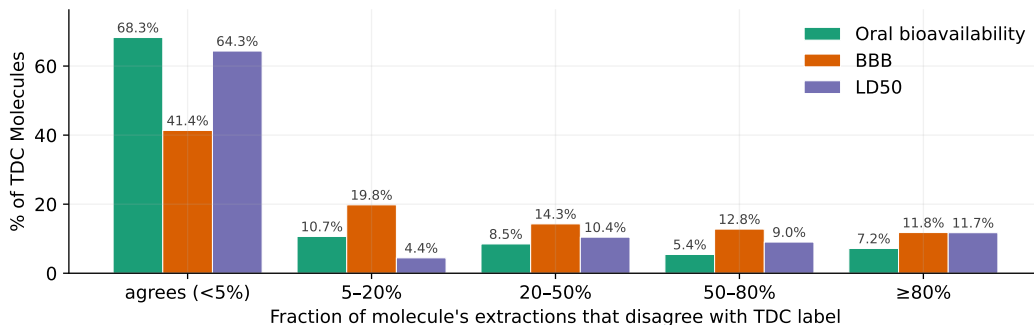


Figure 5: For each labeled molecule in three TDC datasets, what fraction of *Starling*'s extractions disagree with the label? We find that between 12.6% (Oral bioavailability) and 24.6% (BBB) of the labels in TDC are majority disagreed with by the literature.

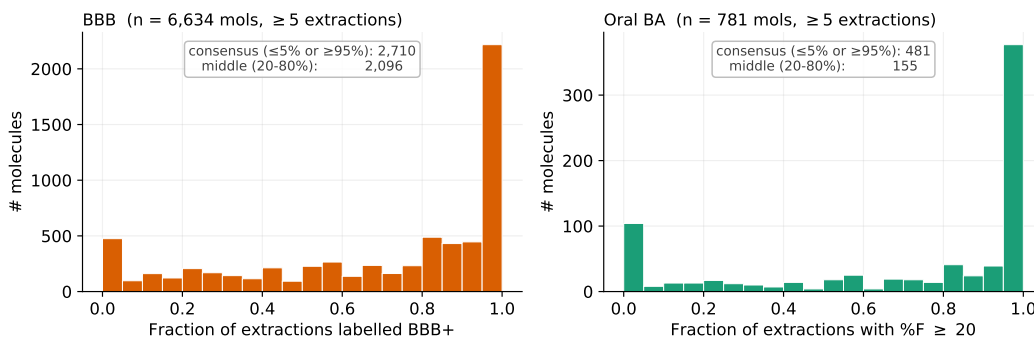


Figure 6: For each molecule with ≥ 5 extractions, what fraction of the extractions would have the + label in the corresponding TDC datasets?

individual labels? In Fig. 5, we take molecules from three TDC datasets and evaluate what fraction of *Starling*'s extractions disagree with the single label for each molecule. We find that, while in two cases the majority of molecules have near-unanimous agreement in the literature, there is a significant tail of disagreement. For example, for BBB we find that 24.6% of molecules in TDC are disagreed with by the majority of literature extractions. These disagreements comprise both errors *and* genuine ambiguity due to context or legitimate biological uncertainty.

In Fig. 6, we show what fraction of the extractions for each *Starling*-extracted molecule with ≥ 5 extractions would have the + label if they were included in the corresponding TDC datasets. Although the fully binary labels (0.0, 1.0) are the mode outcomes, many molecules have substantial disagreement within the literature.